Mon. Not. R. Astron. Soc. **397,** 1464–1485 (2009) doi:10.1111/j.1365-2966.2009.14963.x

r modes and mutual friction in rapidly rotating superfluid neutron stars

B. Haskell,★ N. Andersson and A. Passamonti

School of Mathematics, University of Southampton, Southampton SO17 1BJ

Accepted 2009 April 23. Received 2009 April 23; in original form 2009 February 6

ABSTRACT

We develop a new perturbative framework for studying the r modes of rotating superfluid neutron stars. Our analysis accounts for the centrifugal deformation of the star, and considers the two-fluid dynamics at linear order in the perturbed velocities. Our main focus is on a simple model system where the total density profile is that of an $n = 1$ polytrope. We derive a partially analytic solution for the superfluid analogue of the classical r mode. This solution is used to analyse the relevance of the vortex-mediated mutual friction damping, confirming that this dissipation mechanism is unlikely to suppress the gravitational-wave-driven instability in rapidly spinning superfluid neutron stars. Our calculation of the superfluid r modes is significantly simpler than previous approaches, because it decouples the r mode from all other inertial modes of the system. This leads to the results being clearer, but it also means that we cannot comment on the relevance of potential avoided crossings (and associated 'resonances') that may occur for particular parameter values. Our analysis of the mutual friction damping differs from previous studies in two important ways. First, we incorporate realistic pairing gaps which means that the regions of superfluidity in the star's core vary with temperature. Secondly, we allow the mutual friction parameters to take the whole range of permissible values rather than focusing on a particular mechanism. Thus, we consider not only the weak drag regime, but also the strong drag regime where the fluid dynamics are significantly different.

Key words: gravitational waves – methods: analytical – stars: neutron – stars: oscillations.

1 INTRODUCTION

Oscillations of rapidly rotating neutron stars have attracted interest for a considerable time. During the last decade, significant effort was aimed at understanding whether gravitational-wave emission sets the upper speed limit for pulsars, e.g. via the r-mode instability (Andersson 1998). This possibility is of particular interest since such unstable systems may radiate detectable gravitational waves. In particular, it was suggested that r modes in rapidly rotating neutron stars in low-mass X-ray binaries (LMXBs) may lead to a persistent source of gravitational radiation (Bildsten 1998; Andersson, Kokkotas & Stergioulas 1999b) that may be detected by advanced Laser Interferometer Gravitational-Wave Observatory (LIGO) [see Watts et al. (2008) for the most recent analysis of this problem]. It is of great importance to understand whether internal fluid dissipation allows the instability to develop in such systems or whether it suppresses the r modes completely.

There are, in fact, many mechanisms at work in a real neutron star which compete with the gravitational wave driving of the r mode. One can express the relative strength of these mechanisms in terms of time-scales which will, in general, depend on a large number of parameters. For a basic instability analysis, the most important parameters are the rotation rate and the temperature of the star. The instability can only develop when the gravitational radiation growth time-scale is shorter than the damping time-scales due to the various viscosity mechanisms. This defines a region in the spin-temperature parameter space where the r-mode instability is active. Several studies have been devoted to calculating the shear- and bulk viscosity time-scales for more or less realistic neutron star models. These studies tend to agree that the notion of persistent gravitational-wave emission from accreting neutron stars in LMXBs is quite robust [see Nayyar & Owen (2006) and references therein].

The neutron stars in LMXBs are believed to be old, cold recycled pulsars that have been spun up by accretion. These stars are expected to have superfluid cores and are thus expected to have rather different fluid dynamics and dissipation mechanisms. The simplest description of these systems is provided by a two-fluid model, where the superfluid neutrons are distinguished from the proton–electron plasma (usually treated as a charge-neutral fluid). The oscillations of neutron stars with such superfluid cores have been studied by Lindblom & Mendell (1994) and Andersson & Comer (2001). The latter showed that, as first pointed out by Lee (1995), there are no g modes in such stars, but on

★E-mail: haskellb@soton.ac.uk

the other hand one has a new class of 'superfluid' modes. In particular, there are two families of r modes (Prix, Comer & Andersson 2004). One of these resembles the ordinary r modes of a barotropic star in the sense that the neutrons and protons 'move together'. For the other set of modes, the neutrons and protons are 'counter-moving'. The relative motion of neutrons and protons in a superfluid is, however, rapidly damped by mutual friction, a mechanism that is directly associated with the rotational neutron vortices. The most commonly considered mutual friction mechanism is the scattering of electrons off the magnetic fields associated with the superfluid neutron vortices (Alpar, Langer & Sauls 1984; Andersson, Sidery & Comer 2006). Mutual friction is known to have a decisive impact on neutron star dynamics. In fact, Lindblom & Mendell (1995) have argued that mutual friction completely suppresses the gravitational radiation driven f mode instability [see Andersson, Glampedakis & Haskell (2008) for a recent discussion]. It is thus important to understand if the r-mode instability suffers a similar fate. Previous work on the subject by Lindblom & Mendell (2000) and Lee & Yoshida (2003) presents a somewhat mixed picture. While the ordinary r mode is very weakly damped for most values of the entrainment parameter, the damping becomes very strong for a small range of parameter values. Hence, there may be situations where the mutual friction is strong enough to stop the instability from growing.

The purpose of this paper is to clarify the role of the mutual friction damping and understand whether it can stabilize the r modes against the gravitational-wave instability. In order to do this, we extend the formulation of Andersson et al. (2008) to second order in rotation to calculate the mutual damping time-scale for r modes. Although we do not expect our analysis to lead to results that change previous conclusions, there are good reasons to return to this problem. First of all, previous studies have focused entirely on the weak drag regime for the mutual friction. Meanwhile, recent studies of superfluid turbulence (Peralta et al. 2005, 2006; Andersson, Sidery & Comer 2007), neutron-star-free precession (Glampedakis, Andersson & Jones 2008, 2009) and pulsar glitches (Glampedakis & Andersson 2008) demonstrate that systems in the strong drag regime have very different dynamics. Since one can make convincing arguments for the strong drag regime being relevant (Sedrakian & Sedrakian 1995; Ruderman, Zhu & Chen 1998; Link 2003, 2006), we clearly need to understand the r-mode problem for this parameter range as well. Secondly, we want to improve the treatment of the critical temperature/density at which superfluidity comes into play. The density dependence of the various superfluid pairing gaps translates into distinct regions of normal- and super-fluids that vary with the core temperature. So far, the best analysis in this respect is that of Lindblom & Mendell (2000) who consider a two-fluid core surrounded by a single-fluid envelope. We will build on this by considering superfluid layers, the size of which are determined by a (qualitatively) realistic pairing gap. The size of the superfluid region affects not only the mutual friction but also the shear and bulk viscosities, and it is relevant to demonstrate how this alters the r-mode instability window. Finally, we want to lay the foundation for more detailed work on exotic neutron star cores. It is well established that exotic cores, dominated by either hyperons or deconfined quarks, may be associated with a very strong bulk viscosity (see e.g. Nayyar & Owen 2006). Although it has been suggested that this would lead to the suppression of the r modes, it is clear that such a conclusion is premature. In reality, one would expect superfluidity to play a role. If the hyperons are superfluid, the reactions that produce the bulk viscosity are suppressed and the effect on the r-mode instability may not be that severe (Nayyar & Owen 2006). A similar argument applies to colour superconducting quarks (Alford, Rajagopal & Wilczek 1999). However, it may be important to keep in mind that a superfluid system has extra dynamical degrees of freedom. In order to truly understand the dynamics of these exotic phases of matter, we need to explore the multi-fluid nature of these systems. The present study paves the way for future work in this direction.

2 THE TWO-FLUID EQUATIONS

2.1 The unperturbed problem

Our discussion is based on the usual two-fluid model for neutron star cores (Prix 2004; Andersson & Comer 2006). That is, we consider two dynamical degrees of freedom, loosely speaking, representing the superfluid neutrons (labelled n) and a charge-neutral conglomerate of the protons and electrons (labelled p). Assuming that the individual species are conserved, we have the standard conservation laws

$$\partial_t \rho_{\rm x} + \nabla_i \left(\rho_{\rm x} v_{\rm x}^i\right) = 0, \tag{1}$$

where the constituent index x may be either p or n. The equations of momentum balance can be written as

$$\left(\partial_t + v_{\rm x}^j \nabla_j\right)\left(v_i^{\rm x} + \varepsilon_{\rm x} w_i^{\rm yx}\right) + \nabla_i\left(\tilde{\mu}_{\rm x} + \Phi\right) + \varepsilon_{\rm x} w_{\rm yx}^j \nabla_i v_j^{\rm x} = f_i^{\rm x}/\rho_{\rm x}, \tag{2}$$

where $w_i^{\rm yx} = v_i^{\rm y} - v_i^{\rm x}$ (y ≠ x), and $\tilde{\mu}_{\rm x} = \mu_{\rm x}/m_{\rm x}$ represents the chemical potential (in the following we assume that $m_{\rm p} = m_{\rm n}$). Moreover, Φ represents the gravitational potential, and the parameter $\varepsilon_{\rm x}$ encodes the entrainment effect. The force on the right-hand side of (2) can be used to represent other interactions, including dissipative terms (Andersson & Comer 2006). We will focus on the vortex-mediated mutual friction force for a system that, in equilibrium, rotates uniformly. This means that we consider a force of form (Andersson et al. 2006)

$$f_i^{\rm x} = 2\rho_{\rm n}\mathcal{B}'\epsilon_{ijk}\Omega^j w_{\rm xy}^k + 2\rho_{\rm n}\mathcal{B}\epsilon_{ijk}\hat{\Omega}^j\epsilon^{klm}\Omega_{\rm l} w_m^{\rm xy}. \tag{3}$$

Here, Ω^j is the angular frequency of the neutron fluid (a hat represents a unit vector).

One can express the mutual friction force in terms of a dimensionless 'drag' parameter $\mathcal{R}$ such that (Andersson et al. 2006)

$$\mathcal{B} = \frac{\mathcal{R}}{1+\mathcal{R}^2}, \qquad \text{and} \qquad \mathcal{B}' = \frac{\mathcal{R}^2}{1+\mathcal{R}^2}. \tag{4}$$

In the standard picture, the mutual friction is due to the scattering of electrons off of an array of neutron vortices (Alpar et al. 1984) which leads to $\mathcal{R} \ll 1$, thus placing the problem in the weak drag regime. This means that $\mathcal{B} \ll 1$ and $\mathcal{B}' \ll \mathcal{B}$. Hence, all $\mathcal{B}'$ terms can be neglected.

However, it is commonly thought (Ruderman et al. 1998; Link 2003, 2006) that the strong drag limit, $\mathcal{R} \gg 1$, may apply. Intermediate values for the drag, $\mathcal{R} \approx 1$, are also interesting. In particular, since one would then have both $\mathcal{B} \approx 1$ and $\mathcal{B}' \approx 1$ (note that in the case $\mathcal{R} \gg 1$ one still has $\mathcal{B}' \approx 1$ but $\mathcal{B} \ll 1$). This leads to the presence of terms that may have significant effect on the dynamics of the system (Glampedakis et al. 2008, 2009; Glampedakis & Andersson 2008). At this point, our understanding of neutron star core physics is sufficiently rudimentary that we should avoid ruling out the various possibilities. Hence, we will consider the entire permissible range of values for the drag parameter.

Let us consider a frame rotating with the star at fixed angular velocity Ω^i. The equations of motion then take the form

$$\left(\partial_t + v^j_{\rm x}\nabla_j\right)\left(v^{\rm x}_i + \varepsilon_{\rm x} w^{\rm yx}_i\right) + 2\epsilon_{ijk}\Omega^j v^k_{\rm x} + \nabla_i(\tilde{\mu}_{\rm x} + \Phi_R) + \varepsilon_{\rm x} w^j_{\rm yx}\nabla_i v^{\rm x}_j = f^{\rm x}_i/\rho_{\rm x}, \tag{5}$$

where we have included the centrifugal term in the potential

$$\Phi_R = \Phi - \frac{1}{2}\Omega^2 r^2 \sin^2\theta. \tag{6}$$

The continuity equations maintain the form (1), and the Poisson equation is

$$\nabla^2\Phi = 4\pi G\sum_{\rm x}\rho_{\rm x}. \tag{7}$$

2.2 Perturbations

To keep the problem tractable, we will assume that the background configuration is such that the two fluids rotate together [see Prix et al. (2004), Glampedakis & Andersson (2008) for discussions of oscillations in systems that are not in co-rotation]. Perturbing the equations of motion and working in a frame rotating with Ω^j, we then have

$$\partial_t\left(\delta v^{\rm x}_i + \varepsilon_{\rm x}\delta w^{\rm yx}_i\right) + \nabla_i(\delta\tilde{\mu}_{\rm x} + \delta\Phi) + 2\epsilon_{ijk}\Omega^j\delta v^k_{\rm x} = \delta\left(f^{\rm x}_i/\rho_{\rm x}\right) \tag{8}$$

and

$$\partial_t\delta\rho_{\rm x} + \nabla_j(\rho_{\rm x}\delta v^j_{\rm x}) = 0. \tag{9}$$

To completely specify the perturbation problem, we need boundary conditions. At the centre of the star, we simply require that all variables are regular. The surface of the star is somewhat more complex. In reality, one does not expect the superfluid region to extend all the way to the surface. We shall thus assume that the superfluid is only present in a distinct region determined by the core temperature and the superfluid pairing gap. We will discuss the implementation of this idea once we have set up the relevant system of equations.

From previous work on superfluid neutron star oscillations, e.g. Lindblom & Mendell (1994), Andersson & Comer (2001), Prix & Rieutord (2002), Andersson et al. (2008), we know that the problem has two 'natural' degrees of freedom. One of them represents the total mass flux. Introducing

$$\rho\delta v^j = \rho_{\rm n}\delta v^j_{\rm n} + \rho_{\rm p}\delta v^j_{\rm p} \tag{10}$$

and combining the two Euler equations accordingly, we get

$$\partial_t\delta v^j + \nabla_i\delta\Phi + \frac{1}{\rho}\nabla_i\delta p - \frac{\delta\rho}{\rho^2}\nabla_i p + 2\epsilon_{ijk}\Omega^j\delta v^k = 0, \tag{11}$$

where $\rho = \rho_{\rm n} + \rho_{\rm p}$ and the pressure is obtained from

$$\nabla_i p = \rho_{\rm n}\nabla_i\tilde{\mu}_{\rm n} + \rho_{\rm p}\nabla_i\tilde{\mu}_{\rm p}. \tag{12}$$

We also have

$$\partial_t\delta\rho + \nabla_j(\rho\delta v^j) = 0. \tag{13}$$

At this point, we have two equations which are identical to the perturbation equations for a single-fluid system. Of course, we are considering a two-fluid problem and there is a second dynamical degree of freedom. To describe this, it is natural to consider the difference in velocity. Thus, we introduce

$$\delta w^j = \delta v^j_{\rm p} - \delta v^j_{\rm n}. \tag{14}$$

Combining the two Euler equations in the relevant way, we have

$$(1-\bar{\varepsilon})\partial_t\delta w_i + \nabla_i\delta\beta + 2\bar{\mathcal{B}}'\epsilon_{ijk}\Omega^j\delta w^k - 2\bar{\mathcal{B}}\epsilon_{ijk}\hat{\Omega}^j\epsilon^{klm}\Omega_{\rm l}\delta w_m = 0. \tag{15}$$

We have defined

$$\delta\beta = \delta\tilde{\mu}_{\rm p} - \delta\tilde{\mu}_{\rm n}, \tag{16}$$

which represents the (local) deviation from chemical equilibrium induced by the perturbations. We have also introduced

$$\bar{\varepsilon} = \varepsilon_{\rm n}/x_{\rm p}, \qquad \bar{\mathcal{B}}' = 1 - \mathcal{B}'/x_{\rm p}, \qquad \bar{\mathcal{B}} = \mathcal{B}/x_{\rm p}, \tag{17}$$

and we remind the reader that

$$\rho_{\rm p}\varepsilon_{\rm p} = \rho_{\rm n}\varepsilon_{\rm n}. \tag{18}$$

Finally, we need a second 'continuity' equation. To close the system, it seems natural to consider an equation for the proton fraction $x_{\rm p}$. We then find that

$$\partial_t \delta x_{\rm p} + \frac{1}{\rho}\nabla_j \left[x_{\rm p}(1-x_{\rm p})\rho\delta w^j\right] + \delta v^j \nabla_j x_{\rm p} = 0. \tag{19}$$

2.3 Model equation of state

Let us now consider the set of equations that we have written down. We see that the two degrees of freedom $[\delta v_i, \delta p]$ and $[\delta w_i, \delta\beta]$ only couple 'directly' through (19). For compressible models, the two degrees of freedom also couple "indirectly", since we can use the equation of state to relate $[\delta p, \delta\beta]$ to $[\delta\rho, \delta x_{\rm p}]$.

Deciding to work with δp and $\delta\beta$ [cf. Andersson et al. (2008)], we use

$$\delta\rho = \left(\frac{\partial\rho}{\partial p}\right)_\beta \delta p + \left(\frac{\partial\rho}{\partial\beta}\right)_{\rm p} \delta\beta \tag{20}$$

and

$$\delta x_{\rm p} = \left(\frac{\partial x_{\rm p}}{\partial p}\right)_\beta \delta p + \left(\frac{\partial x_{\rm p}}{\partial\beta}\right)_{\rm p} \delta\beta. \tag{21}$$

As a simple model, we shall consider an equation of state such that

$$\left(\frac{\partial\rho}{\partial p}\right) = \frac{1}{c_{\rm s}^2} \tag{22}$$

where $c_{\rm s}$ is the background sound speed. We combine this with a simple linear expression for the proton fraction

$$x_{\rm p} = \alpha\rho. \tag{23}$$

This leads to

$$\left(\frac{\partial x_{\rm p}}{\partial p}\right) = \frac{\alpha}{c_{\rm s}^2} \quad \text{and} \quad \left(\frac{\partial x_{\rm p}}{\partial\beta}\right) = \frac{\alpha^2\rho^2}{c_{\rm s}^2} \tag{24}$$

where we have used the relation (Andersson & Comer 2001)

$$\left(\frac{\partial\rho}{\partial\beta}\right) = \rho^2 \left(\frac{\partial x_{\rm p}}{\partial p}\right) \tag{25}$$

to get

$$\left(\frac{\partial\rho}{\partial\beta}\right) = \frac{\alpha\rho^2}{c_{\rm s}^2}. \tag{26}$$

In our model calculations, we shall take $\alpha = 6\times10^{-3}/\rho_{\rm nuc}$ where $\rho_{\rm nuc} \approx 2.8\times10^{14}$ g cm^{-3} is the nuclear saturation density.

In a superfluid system, the momentum of each component may not be parallel to its velocity. Rather, it acquires a component along the relative velocity. This is evident from equation (2). This non-dissipative coupling is usually parametrized in terms of the entrainment parameter $\varepsilon_{\rm x}$. One can show (Prix et al. 2004) that this parameter is linked to the effective proton mass, $m_{\rm p}^*$, according to

$$\varepsilon_{\rm p} = 1 - \frac{m_{\rm p}^*}{m_{\rm p}}. \tag{27}$$

For simplicity, we shall take $\varepsilon_{\rm p}$ to be constant throughout the superfluid region of the star. Recent work suggests that, while this may not be a good approximation for an entire neutron star, it is approximately true if we consider a shell. From Chamel (2008), we see that a reasonable range for the entrainment parameter is $\varepsilon_{\rm p} \approx 0.2$–$0.8$.

In order to compare our results to previous work, it is worth recalling that the entrainment parameter ϵ used by Lindblom & Mendell (2000) is related to $\varepsilon_{\rm p}$ by

$$\epsilon = \frac{\varepsilon_{\rm p} x_{\rm p}}{1 - x_{\rm p} - \varepsilon_{\rm p}}. \tag{28}$$

Hence, their range of $\epsilon \approx 0.02$–0.06 corresponds, if we take a volume average of $x_{\rm p}$, to $\varepsilon_{\rm p} \approx 0.45$– 0.85.

To summarize, when we solve the r-mode problem, we will consider an equation of state represented by (i) the overall density profile, represented by the sound speed $c_{\rm s}^2$, (ii) the proton fraction $x_{\rm p}$ and (iii) the entrainment parameter $\varepsilon_{\rm p}$. These quantities allow us to specify the background needed for the perturbation problem. This model is quite simplistic, and it would not be difficult to make it more realistic. However, our main interest is to explore how the r-mode results depend on the different parameters. This question is easier to address with a simple parametrized model.

3 SLOW-ROTATION ANALYSIS

In order to determine the rotational corrections to the superfluid r modes, we will apply the formalism of Saio (1982) to the problem. Thus, we consider corrections up to the order of $O(\Omega^2)$ in the slow-rotation approximation. We will also make the Cowling approximation, i.e. neglect perturbations of the gravitational potential, $\delta\Phi$.

We start by considering a slowly, and uniformly, rotating star. It is well known that such a star will not be spherical and that a distorted potential surface can be written in the form

$$r = a[1 + \epsilon(a, \theta)]. \tag{29}$$

Here, ϵ is a function of a and θ which represents the deformation of the equilibrium structure from the background spherical state. The equilibrium physical quantities are functions only of a. Following Saio (1982) and Smeyers & Martens (1983), we write the equations of motion in a frame corotating with the star, denoted by $\{q^i\}$, starting from a static Cartesian frame, denoted by $\{x^i\}$. Our coordinates in the rotating frame will be a spherical polar system, explicitly

$$x^1 = a(1 + \epsilon)\sin\theta\cos(\phi + \Omega t) \tag{30}$$

$$x^2 = a(1 + \epsilon)\sin\theta\sin(\phi + \Omega t) \tag{31}$$

$$x^3 = a(1 + \epsilon)\cos\theta. \tag{32}$$

The metric in the new coordinates is then given by

$$g_{ab} = \delta_{ij}\frac{\partial x^i}{\partial q^a}\frac{\partial x^j}{\partial q^b} \tag{33}$$

which, after linearizing with respect to ϵ, leads to

$$g_{ab} = \left\{\begin{array}{ccc} 1 + 2\epsilon + 2a\frac{\partial\epsilon}{\partial a} & a\frac{\partial\epsilon}{\partial\theta} & 0 \\ a\frac{\partial\epsilon}{\partial\theta} & a^2(1 + 2\epsilon) & 0 \\ 0 & 0 & a^2(1 + 2\epsilon)\sin^2\theta \end{array}\right\} + O(\epsilon^2). \tag{34}$$

The connection coefficients, in the coordinate basis

$$\left\{e_a = \frac{\partial}{\partial a}, e_\theta = \frac{\partial}{\partial\theta}, e_\phi = \frac{\partial}{\partial\phi}\right\}, \tag{35}$$

can be obtained from

$$\Gamma^a_{bc} = \frac{1}{2}g^{ad}(g_{bd,c} + g_{cd,b} - g_{bc,d}). \tag{36}$$

We shall, however, use the vector basis

$$\{\hat{e}_i\} = \left\{\hat{e}_a = \frac{\partial}{\partial a}, \hat{e}_\theta = \frac{1}{a}\frac{\partial}{\partial\theta}, \hat{e}_\phi = \frac{1}{a\sin\theta}\frac{\partial}{\partial\phi}\right\} \tag{37}$$

for which the covector basis is

$$\left\{\hat{\omega}^i\right\} = \{da, ad\theta, a\sin\theta d\phi\}. \tag{38}$$

Note that the basis vectors are not orthogonal.

Before we proceed, it is worth recalling that Smeyers & Martens (1983) have argued that the derivation of Saio's results is flawed, even though the final results for the rotational frequency correction are correct. Since this is an important point, we will outline how the second-order slow-rotation perturbation equations should be derived following Saio's strategy.

As we are considering linear perturbations on a rotationally distorted background, the first step is to calculate such a background, using the coordinates (a, θ, ϕ) defined above. The equations that govern the background equilibrium are particularly simple (if we assume that neutrons and protons do not move relative to each other)

$$\frac{1}{\rho(a)}\frac{\mathrm{d}P(a)}{\mathrm{d}a} = -\frac{\mathrm{d}\Phi_R(a)}{\mathrm{d}a} \tag{39}$$

where Φ_R, defined in equation (6), includes the centrifugal terms. This is due to the fact that the coordinate a has been defined in such a way as to label the equipotential surfaces of Φ_R, which are also isobaric (and isopycnic as the background equation of state is barotropic) surfaces of the star, thus leading to all the background quantities being a function of a only [for a detailed description see Tassoul (1978)]. The Euler equations are thus identical to those one would obtain for a spherical background and the solution can be formally obtained by replacing the radial coordinate r with the variable a in the spherically symmetric solution. It is important to remember, however, that we are calculating physical quantities at a point P in the deformed star labelled by the coordinates (a, θ, ϕ) and not at a point P_0 in the spherical star labelled by coordinates $(r = a, \theta, \phi)$. Note, in fact, that as the geometry is not spherical the measures of distance and volume change. For example, the mass of the star is now obtained from

$$M = \int_{a=0}^{R}\int_{\theta=0}^{\pi}\int_{\phi=0}^{2\pi}\rho(a)a^2\sin\theta\left[1 + 3\epsilon(a, \theta) + a\frac{d\epsilon(a, \theta)}{\mathrm{d}a}\right]\mathrm{d}a\ \mathrm{d}\theta\ \mathrm{d}\phi = M_0 + \delta M_\Omega \tag{40}$$

where M_0 is the mass of the spherically symmetric star and δM_Ω is the difference in mass due to rotation.

3.1 Perturbations

Let us now consider linear perturbations on our rotationally deformed background. We shall express the perturbations in terms of a total displacement vector ξ^+_i, such that $\delta v_i = i\sigma\xi^+_i$, and a difference displacement vector ξ^-_i, such that $\delta w_i = i\sigma\xi^-_i$. We can then write equation (11)

as

$$\sigma^2 \xi_i^+ - \frac{1}{\rho}\nabla_i^0 \delta P + \frac{\delta\rho}{\rho^2}\delta_{ia}\frac{dP}{da} + i\sigma C_i^+ = 0, \tag{41}$$

where the δ that denotes the Eulerian perturbations should not be confused with the Kronecker delta δ_{ia}. We are using $i\sigma C_i^+$ to represent the Coriolis force, and the vector $C_i^\pm$ has the following components:

$$C_a^\pm = 2\Omega\left(1 + 2\epsilon + a\frac{\partial\epsilon}{\partial a}\right)\sin\theta\xi_\pm^\phi \tag{42}$$

$$C_\theta^\pm = 2\Omega\left(1 + 2\epsilon + \tan\theta\frac{\partial\epsilon}{\partial a}\right)\cos\theta\xi_\pm^\phi \tag{43}$$

$$C_\phi^\pm = 2\Omega\left[\xi_\pm^a \sin\theta\left(1 + 2\epsilon + a\frac{\partial\epsilon}{\partial a}\right) + \xi_\pm^\theta\left(1 + 2\epsilon + \tan\theta\frac{\partial\epsilon}{\partial\theta}\right)\right]. \tag{44}$$

The differential operator ∇_i^0 is the same as for spherical polar coordinates, i.e.

$$\nabla_i^0 \xi^i = \frac{1}{a^2}\frac{\partial(a^2\xi^a)}{\partial a} + \frac{1}{a\sin\theta}\frac{\partial(\sin\theta\xi^\theta)}{\partial\theta} + \frac{1}{a\sin\theta}\frac{\partial\xi^\phi}{\partial\phi}. \tag{45}$$

The continuity equation (13) becomes

$$\delta\rho + \nabla_0^i\left(\rho\xi_i^+\right) + \rho\xi_i^+\nabla_0^i\left(3\epsilon + a\frac{\partial\epsilon}{\partial a}\right) = 0. \tag{46}$$

We shall also need the linearized equation of state. In our model case, we have

$$\Gamma = \frac{c_{\rm s}^2 p}{\rho}. \tag{47}$$

That is, in comparing our equations to Saio's results one should only consider the barotropic limit.

Let us now consider the equations that govern the second degree of freedom, the difference in velocity. Equation (15) takes the form

$$\sigma^2(1-\bar{\varepsilon})\xi_i^- - \nabla_i^0\delta\beta + i\sigma\bar{\mathcal{B}}'C_i^- + i\sigma\bar{\mathcal{B}}G_i = 0 \tag{48}$$

where G_i has the following components:

$$G_a = \Omega\left[\left(1 + 2\epsilon + 2a\frac{\partial\epsilon}{\partial a}\right)\sin\theta^2\xi_-^a + \left(1 + 2\epsilon + a\frac{\partial\epsilon}{\partial a} + \tan\theta\frac{\partial\epsilon}{\partial\theta}\right)\cos\theta\sin\theta\xi_-^\theta\right] \tag{49}$$

$$G_\theta = \Omega\left[\left(1 + 2\epsilon + 2\tan\theta\frac{\partial\epsilon}{\partial\theta}\right)\cos\theta^2\xi_-^\theta + \left(1 + 2\epsilon + a\frac{\partial\epsilon}{\partial a} + \frac{\partial\epsilon}{\partial\theta} - \cot\theta\frac{\partial\epsilon}{\partial\theta}\right)\cos\theta\sin\theta\xi_-^a\right] \tag{50}$$

$$G_\phi = \Omega(1 + 2\epsilon)\,\xi_-^\phi. \tag{51}$$

Finally, we find that the second continuity equation (19) takes the form

$$\delta x_{\rm p} + \frac{1}{\rho}\nabla_0^i\left[x_{\rm p}(1-x_{\rm p})\rho\xi_i^-\right] + x_{\rm p}(1-x_{\rm p})\xi_i^-\nabla_0^i\left(3\epsilon + a\frac{\partial\epsilon}{\partial a}\right) + \xi_i^+\nabla_0^i x_{\rm p} = 0. \tag{52}$$

4 THE R-MODE PROBLEM

We are mainly interested in understanding the effect that mutual friction has on the r-mode instability. It is well-known that the r modes have zero frequency and are purely axial in the non-rotating limit. Rotation breaks this degeneracy and leads to modes that are purely axial to leading order but which have a poloidal component of order $O(\Omega^2)$. These modes have frequency

$$\sigma_r = \sigma_0\Omega + \sigma_2\Omega^3. \tag{53}$$

The r-mode frequency can be calculated, to second order in rotation, for a single-fluid star using a number of different formalisms (Andersson, Kokkotas & Schutz 1999a; Lindblom, Mendell & Owen 1999; Yoshida & Lee 2000). The superfluid problem has been solved both to linear (Andersson & Comer 2001; Prix et al. 2004; Andersson et al. 2008) and to second (Lindblom & Mendell 2000; Lee & Yoshida 2003) order in rotation. To leading order, one finds that the ordinary r mode has frequency

$$\sigma_0 = \frac{2m\Omega}{l(l+1)} \tag{54}$$

where, in fact, only the $l = m$ modes exist. In addition, a constant density model supports a set of purely axial counter-moving modes with frequency (Andersson et al. 2008)

$$\sigma_0 = \frac{2m\Omega}{l(l+1)(1-\bar{\varepsilon})}\left\{\bar{\mathcal{B}}' + i\bar{\mathcal{B}}\frac{[l(l+1)-m^2]}{m}\right\}. \tag{55}$$

Since the frequency in (55) contains the term $(1-\bar{\varepsilon})$, it is easy to see that it can only be the solution for a global mode if $\bar{\varepsilon} = \varepsilon_{\rm p}/(1-x_{\rm p})$ is constant. In the present analysis, we will assume that $\varepsilon_{\rm p}$ is constant. Hence, the second class of r modes can only exist if we also assume that the proton fraction $x_{\rm p}$ is constant. If $x_{\rm p}$ is constant, the co-rotating and counter-rotating degrees of freedom are, in fact, completely decoupled also at second order in rotation. The r mode is then exactly the same as for a barotropic single-fluid star. In particular, r-mode solutions exist only for $l = m$. However, we are not generally considering a constant $x_{\rm p}$ (in fact, we are assuming that the proton fraction scales linearly with the total mass density, which is not constant). Hence, we see that there will be no counter-moving r modes in our model. In fact, if $x_{\rm p}$ is not a constant, then the coupling between the degrees of freedom leads to the counter-moving r mode becoming a general inertial mode, with a mixed toroidal/poloidal velocity field to leading order. These modes have been determined numerically by Lee & Yoshida (2003). If we consider a generic profile for $x_{\rm p}$ and work at second order in rotation, the leading order r mode will drive the counter-moving degrees of freedom, leading to mutual friction damping. This is the effect that we are interested in.

4.1 Perturbation equations

So far, we have written down the equations for a general perturbation problem on the rotationally deformed background. We will now focus on modes that are purely toroidal to leading order. That is, we write the total displacement vector as

$$\frac{\xi^i_+}{a} = \left(0, \frac{K_{lm}}{\sin\theta}\frac{\partial}{\partial\phi}, -K_{lm}\frac{\partial}{\partial\theta}\right)Y^m_l + \sum_{\nu,\mu}\left(S_{\nu\mu}, Z_{\nu\mu}\frac{\partial}{\partial\theta}, \frac{Z_{\nu\mu}}{\sin\theta}\frac{\partial}{\partial\phi}\right)Y^\mu_\nu. \tag{56}$$

Analogously, the difference displacement vector can be written as

$$\frac{\xi^i_-}{a} = \left(0, \frac{k_{lm}}{\sin\theta}\frac{\partial}{\partial\phi}, -k_{lm}\frac{\partial}{\partial\theta}\right)Y^m_l + \sum_{\nu,\mu}\left(s_{\nu\mu}, z_{\nu\mu}\frac{\partial}{\partial\theta}, \frac{z_{\nu\mu}}{\sin\theta}\frac{\partial}{\partial\phi}\right)Y^\mu_\nu. \tag{57}$$

Note that we use uppercase variables for the comoving degree of freedom and the corresponding lowercase variable for the counter-moving degree of freedom.

As noted by Smeyers & Martens (1983), the above form for the displacement vectors does not correspond to the usual decomposition in spheroidal and toroidal components. At second order in rotation, the above basis differs from the standard basis on a spherical background as the vector $\hat{e}_a$ is no longer orthogonal to $\hat{e}_\theta$. This is, however, not a problem as we do not need to explicitly identify the poloidal and toroidal parts of the mode at second order in rotation. Such an identification would not be very useful anyway since the components are coupled at $O(\Omega^2)$.

We want to study the classical r mode, i.e. a mode that to first order in rotation involves only the comoving degree of freedom and which is purely toroidal in the slow-rotation limit. This identification is unique since our decomposition coincides with the standard one into poloidal and toroidal components at $O(\Omega)$. The requirement is that the leading term K_{lm} is of the order of unity while the amplitudes of the 'spheroidal' components are of the order of Ω^2 for the total displacement. Meanwhile, following the first order results of Andersson et al. (2008), all components of the difference displacement must be of the order of Ω^2. As discussed in Appendix A, this ordering for the displacement vector, together with the frequency from equation (53), leads to the following equations for the $l = m$ r modes:

$$a\frac{dS_{l+1}}{da} = \left(\frac{V}{\Gamma} - 3\right)S_{l+1} - \frac{V}{\Gamma}\zeta_{l+1} + (l+1)(l+2)Z_{l+1} + 3im\,Q_{l+1}K_{lm}\left(3D_2 + a\frac{dD_2}{da}\right) \tag{58}$$

$$a\frac{d\zeta_{l+1}}{da} = (1-U)\zeta_{l+1} - \frac{V}{\Gamma}x_{\rm p}\tau_{l+1} - 2ic_1\omega\tilde{\omega}l\,Q_{l+1}K_{lm} \tag{59}$$

$$a\frac{ds_{l+1}}{da} = (X-3)\,s_{l+1} - \zeta_{l+1}\frac{1}{x_{\rm p}(1-x_{\rm p})}\frac{V}{\Gamma} + (l+1)(l+2)z_{l+1} - CS_{l+1} + 3im\,Q_{l+1}k_{lm}\left(3D_2 + a\frac{dD_2}{da}\right) \tag{60}$$

$$\begin{aligned} a\frac{d\tau_{l+1}}{da} = {} & (1-U)\tau_{l+1} - 2c1\omega\tilde{\omega}Q_{l+1}k_{lm}\left(il\bar{\mathcal{B}}' - m\bar{\mathcal{B}}\right) - 2c_1\omega\tilde{\omega}z_{l+1}\left[m\bar{\mathcal{B}}' + i\bar{\mathcal{B}}\left((l+1)Q^2_{l+2} - (l+2)Q^2_{l+1}\right)\right] \\ & + c_1\omega s_{l+1}\left[\omega(1-\bar{\varepsilon}) + 2i\tilde{\omega}\bar{\mathcal{B}}\left((Q^2_{l+2} + Q^2_{l+1}) - 1\right)\right] \end{aligned} \tag{61}$$

$$\zeta_{l+1} = -2i\omega\tilde{\omega}c_1\frac{l}{l+1}Q_{l+1}K_{lm} \tag{62}$$

$$\begin{aligned} \tau_{l+1}(l+1)(l+2) = {} & -2i\bar{\mathcal{B}}'\omega\tilde{\omega}c_1 l(l+2)Q_{l+1}k_{lm} + 2m(l+2)\bar{\mathcal{B}}\omega\tilde{\omega}c_1 Q_{l+1}k_{lm} \\ & + c_1\omega z_{l+1}\left\{\omega(l+1)(l+2)(1-\bar{\varepsilon}) - 2m\tilde{\omega}\bar{\mathcal{B}}' - 2i\tilde{\omega}\bar{\mathcal{B}}\left[m^2 + Q^2_{l+2}(l+1)(l+4) + Q^2_{l+1}(l+2)(l-1)\right]\right\} \\ & - 2c_1\omega\tilde{\omega}s_{l+1}\left\{m\bar{\mathcal{B}}' - i\bar{\mathcal{B}}\left[Q^2_{l+2}(l+4) - Q^2_{l+1}(l-1) - 1\right]\right\} \end{aligned} \tag{63}$$

where

$$K_{lm} = -\frac{i\omega_0}{me} l Q_{l+1} \left[S_{l+1} + (l+2) Z_{l+1} \right] \tag{64}$$

$$k_{lm} = \frac{\omega_0}{m\eta} \left(m\bar{\mathcal{B}} - il\bar{\mathcal{B}}' \right) Q_{l+1} \left[s_{l+1} + (l+2) z_{l+1} \right]. \tag{65}$$

In the last two expressions, we have used

$$e = (\omega - \omega_0) + 3D_2 \left\{ \frac{2\omega}{l(l+1)} \left[l Q_{l+1}^2 \right] - \omega_0 \left[5Q_{l+1}^2 - 1 \right] \right\} \tag{66}$$

$$\eta = (1 - \bar{\varepsilon})(\omega_0 - \omega_1). \tag{67}$$

It is easy to verify that these equations coincide with the results of Saio (1982) in the barotropic limit. In fact, in order to facilitate this comparison, we have used essentially the same notation as Saio. Thus, we have defined the normalized mode frequency

$$\omega = \sigma \left(\frac{R^3}{GM} \right)^{1/2} \tag{68}$$

and the following background quantities:

$$M_r = 4\pi \int_0^a \rho a^2 \, \mathrm{d}a \tag{69}$$

$$U = \frac{\mathrm{d} \log M_r}{\mathrm{d} \log a} \tag{70}$$

$$V = -\frac{\mathrm{d} \log P}{\mathrm{d} \log a} \equiv \frac{ga\rho}{P} \tag{71}$$

$$c_1 = \left(\frac{a}{R} \right)^3 \frac{M}{M_r} \tag{72}$$

$$\tilde{\omega} = \Omega \left(\frac{R^3}{GM} \right)^{1/2} \tag{73}$$

$$X = -\frac{\mathrm{d} \log \left[\rho x_\mathrm{p} (1 - x_\mathrm{p}) \right]}{\mathrm{d} \log a} \tag{74}$$

$$C = \frac{a}{x_\mathrm{p}(1 - x_\mathrm{p})} \frac{\mathrm{d}x_\mathrm{p}}{\mathrm{d}a} \tag{75}$$

$$\epsilon = D_1(a) + D_2(a) P_2(\cos\theta) \tag{76}$$

where $P_2(\cos\theta)$ is the Legendre polynomial:

$$P_2(\cos\theta) = (3\cos^2\theta - 1)/2. \tag{77}$$

We are also using the definition

$$Q_l = \left[\frac{(l-m)(l+m)}{(2l+1)(2l-1)} \right]^{1/2}. \tag{78}$$

For later convenience, it is worth noting that this means that $Q_m = 0$.

4.2 Rotating $n = 1$ polytropes

We will now restrict ourselves to the case where the density profile of the equilibrium configuration is that of an $n = 1$ polytrope. This greatly simplifies the analysis, as the background quantities we are interested in can be obtained in closed form. Explicitly, we have

$$p = K\rho^2 \tag{79}$$

with

$$K = \frac{2GR^2}{\pi}. \tag{80}$$

Introducing the dimensionless variable $y = \pi a/R$, we then find that

$$\rho = \frac{\pi M_0}{4R^3} \frac{\sin y}{y} \tag{81}$$

from which we can define

$$M_r = \frac{M_0}{\pi}[\sin y - y\cos y]. \tag{82}$$

Furthermore, we can calculate, following the classical work of Chandrasekhar (1933), the rotationally induced deformation

$$D_1 = \tilde{D}_1\tilde{\omega}^2 = \frac{2}{\pi^2}\frac{M_0 a\psi_1}{RM_r}\tilde{\omega}^2 \tag{83}$$

and

$$D_2 = \tilde{D}_2\tilde{\omega}^2 = -\frac{1}{9}\frac{M_0 a\psi_2}{RM_r}\tilde{\omega}^2 \tag{84}$$

where

$$\psi_1 = 1 - \frac{\sin y}{y} \tag{85}$$

$$\psi_2 = \frac{15}{y}\left[\left(\frac{3}{y^2} - 1\right)\sin y - \frac{3}{y}\cos y\right]. \tag{86}$$

The mass of the star is thus, from equation (40), given by

$$M = M_0\left[1 + \frac{2}{\pi^2}\tilde{\omega}^2\left(\frac{\pi^2}{3} - 1\right)\right]. \tag{87}$$

In the following, when we quote the mass of the star we shall in fact be referring to the mass of the spherical star, M_0. Formally, what we are doing is thus considering a sequence of stellar models with the same central density, but with a mass that varies with the rotation rate. The difference in mass does not, however, enter the r-mode frequency correction to the order of $O(\Omega^3)$ and is thus irrelevant for the present discussion.

Finally, we will also need the sound speed, which simply follows from

$$c_{\rm s}^2 = 2K\rho. \tag{88}$$

4.3 Decoupling the degrees of freedom

Let us now examine the consequences of the ordering we assumed at the beginning of the analysis. From equation (62), we see that if K_{lm} is of the order of unity then ζ_{lm} (i.e. the pressure perturbation) must be of the order of Ω^2. Similarly, from equation (63) we see that, as all components of the difference displacement are of the order of Ω^2, the variable τ_{lm} (i.e. $\delta\beta$) must be of the order of Ω^4. It follows that in equation (59) the term involving τ_{lm} is of higher order than the others and can be neglected. The consequence of this is that the equations for the comoving degree of freedom are *completely decoupled*. Hence, they can be solved independently and then used as source terms for the counter-moving degrees of freedom. This approach has obvious advantages compared to previous fully numerical calculations (Lindblom & Mendell 2000; Lee & Yoshida 2003). After all, we can now solve for the r mode throughout the star, imposing regularity at the centre of the star and the vanishing of the Lagrangian perturbation of the pressure, Δp, at the surface. As a second independent step, we solve the equations for the counter-moving degree of freedom. Adopting this strategy, it becomes straightforward to account for, for example, the temperature dependence of the superfluid gap and the associated variation of the superfluid region in the star.

The solution for the comoving degree of freedom is particularly simple. Not only is it decoupled from the counter-moving degree of freedom, the equation for ζ_{lm} also decouples and takes the form:

$$a\frac{{\rm d}\zeta_{l+1}}{{\rm d}a} = (l + 2 - U)\zeta_{l+1} \tag{89}$$

leading to the solution

$$\frac{\zeta_{l+1}}{a} = 2\frac{\omega\tilde{\omega}}{\sqrt{2l+3}}\frac{l}{l+1}\frac{M_0}{M_r R}\left(\frac{a}{R}\right)^{l+1} = B\frac{a^{l+1}}{M_r}. \tag{90}$$

One can use this solution to determine S_{l+1} from equation (58). This leads to

$$a\frac{{\rm d}S_{l+1}}{{\rm d}a} + (l + 4 - V_g)S_{l+1} = -(V_g + h)\zeta_{l+1} \tag{91}$$

where $V_g = V/\Gamma$ and (for the $l = m$ modes we are considering)

$$h = \frac{1}{\omega_0^2}\frac{M(a)}{M}\left(\frac{R}{a}\right)^3\left[\frac{(l+1)(2l+3)e}{K\omega_0} + 3\left(3D_2 + a\frac{dD_2}{da}\right)\right] \tag{92}$$

with e defined in equation (A27). To solve equation (91) let us first of all consider the solution to the homogeneous problem. This is readily obtained and takes the form

$$S_{l+1} = \frac{C}{p^{1/\Gamma}a^{l+4}}. \tag{93}$$

where C is a constant.

Note that this solution diverges both at the centre and at the surface of the star. We next need to determine a particular solution to the problem. To do this, let us write h as

$$h = \left(\frac{R}{a}\right)\frac{M(a)}{M}(\tilde{h}_{\rm c} + \tilde{h}_a) \tag{94}$$

where

$$\tilde{h}_{\rm c} = \frac{(l+1)(2l+3)\omega_2}{l\sigma_0^3} \tag{95}$$

$$\tilde{h}_a = \frac{3}{\sigma_0}\left[(2l+3)\tilde{D}_2 + a\frac{d\tilde{D}_2}{da}\right]. \tag{96}$$

Inspired by the solution to the homogeneous problem, we make the following ansatz for the particular solution to (91):

$$S_{l+1} = \frac{f(a)}{p^{1/\Gamma}a^{l+4}}. \tag{97}$$

This leads to

$$\frac{{\rm d}f}{{\rm d}a} = -(V_g + h)p^{1/\Gamma}a^{L+3}\zeta_{l+1}. \tag{98}$$

The first term is thus of the form

$$V_g p^{1/\Gamma}a^{m+3}\zeta_{l+1} = BG\frac{a^{2l+4}}{\Gamma\sqrt{K}}, \tag{99}$$

which is easily integrated. For the second part, we need to be able to integrate, for the term proportional to $\tilde{h}_{\rm c}$,

$$\tilde{h}_{\rm c}p^{1/\Gamma}a^{l+3}\zeta_{l+1} = B\sqrt{K}\tilde{h}_{\rm c}\frac{R^3}{M}\rho a^{2l+2} \tag{100}$$

so that, for an $n = 1$ polytrope, we require

$$\int_0^a \rho x^{2l+2}{\rm d}x = \frac{\pi M}{4R^3}\left(\frac{R}{\pi}\right)^{2l+3}\int_0^{\pi a/R} y^{2l+1}\sin y\,{\rm d}y = \frac{\pi M}{4R^3}\left(\frac{R}{\pi}\right)^{2l+3}\mathcal{I}_1(y). \tag{101}$$

For the remaining part, involving $\tilde{h}_a$, we require the integral

$$\mathcal{I}_2 = 3\int \rho a^{2l+2}\left[(2l+3)\tilde{D}_2 + a\frac{{\rm d}\tilde{D}_2}{{\rm d}a}\right] \tag{102}$$

which, using the explicit form for D_2 in equation (84), gives

$$\mathcal{I}_2 = -\frac{5MR^{2l}}{4\pi^{2l+2}}[f_1(y) + f_2(y)] \tag{103}$$

where

$$f_1(y) = \frac{y^{2l}\sin y}{\sin y - y\cos y}[(3-y^2)\sin y - 3y\cos y] \tag{104}$$

$$f_2(y) = \int_0^y x^{2l-1}[(3-x^2)\sin x - 3x\cos x]\,{\rm d}x. \tag{105}$$

This analysis is perhaps a little bit messy, but the result is very useful. Collecting the various results, we can write the final solution to equation (98) as

$$f(y) = -\frac{BG}{\sqrt{K}}\left(\frac{R}{\pi}\right)^{2l+5}\left\{\frac{y^{2l+5}}{2(2l+5)} + \frac{\pi^2}{16}\frac{(l+1)^4(2l+3)}{l}\sigma_2\mathcal{I}_1(y) - \frac{5\pi^2(l+1)^2}{8}[f_1(y) + f_2(y)]\right\}. \tag{106}$$

That is, we have an analytic solution to the problem.

As we now have the full solution to the problem, we can impose boundary conditions. First of all, we require the solution to be regular at the centre of the star. This determines the constant $C = 0$ in the homogeneous solution. The remaining condition is that the Lagrangian variation of the pressure vanishes at the surface of the star, which in terms of our variables means that

$$\Delta p = \rho g a\sum[\zeta_{l+1} - S_{l+1}]Y^l_{l+1} \to 0 \quad \text{as} \quad a \to 0. \tag{107}$$

Given that our equation of state is such that $\rho \to 0$ at the surface, we simply require ζ_{l+1} and S_{l+1} to be regular. This means that we must have

$$f(\pi) = 0. \tag{108}$$

Conveniently, this leads to an algebraic formula for the rotational frequency correction σ_2,

$$\sigma_2 = -\frac{16}{\pi^2}\frac{l}{(l+1)^4(2l+3)}\left[\frac{\pi^{2l+5}}{2(2l+5)} - \frac{5\pi^2(l+1)^2}{8}f_2(\pi)\right]\frac{1}{\mathcal{I}_2}. \tag{109}$$

The determined frequency corrections for the first few values of l are listed in Table 1. These results are in good agreement with the numerical results of Lindblom et al. (1999), within a few per cent for $l > 2$. The greatest difference is approximately 10 per cent for the $l = m = 2$

Table 1. r-mode frequency corrections at second order in the slow-rotation approximation. The quantity σ_2 is defined by the relation $\sigma = \sigma_0\Omega + \sigma_2\Omega^3$ and, for the $l = m$ case that we are considering, $\sigma_0 = 2\Omega/(l + 1)$. These results are in good agreement with the results of Lindblom et al. (1999), within a few per cent for $l > 2$, the greatest difference is approximately 10 per cent for the $l = m = 2$ mode. These differences are most likely due to our use of the Cowling approximation. In fact, for the $l = m = 2$ mode our frequency agrees to within a few per cent with that obtained with the numerical code of Passamonti et al. (2008), in which the Cowling approximation is made, and to better than 1 per cent with the results of Andersson and Kokkotas (2001).

l	σ_0	σ_2
1	1.000	0.3033
2	0.666	0.4525
3	0.500	0.4429
4	0.400	0.4051
5	0.333	0.3659
6	0.286	0.3310
7	0.250	0.3010
8	0.222	0.2754
9	0.200	0.2535
10	0.182	0.2346

mode. The discrepancy should be entirely due to our use of the Cowling approximation. In fact, for the $l = m = 2$ mode our frequency agrees to within a few per cent with that obtained with the numerical code of Passamonti, Haskell & Andersson (2008). Our results also agree well, with errors smaller than 1 per cent, with the previous Cowling approximation result of Andersson & Kokkotas (2001).

4.4 The superfluid degree of freedom

At this point, we have reached two interesting conclusions. First of all, we have found that the rotational corrections for the r mode can be obtained in closed form for $n = 1$ polytropes (in the Cowling approximation). This analytic solution will undoubtedly help us understand the nature of the r modes and the effect of different dissipation channels better. The second result concerns the fact that the superfluid, counter-moving, degree of freedom remains uncoupled also at this order of approximation. This is obvious since the frequency correction to the order of Ω^3 could be calculated without determining the counter-moving eigenfunctions. These are, in fact, only needed if we want to calculate the frequency correction to order Ω^5. As we shall see in the following, this is exactly the order at which the mutual friction damping corrections appear explicitly in the frequency.

To complete the r-mode solution at the current level of approximation, we need to use the analytic solution to the comoving problem to provide the source terms in equations (A5) and (A6) for the counter-moving degrees of freedom. When we consider this problem, it becomes apparent that the decoupling of the two degrees of freedom is advantageous. In fact, it is now straightforward to study neutron stars with different models of superfluidity. This is an important improvement on previous work in this area, where it has generally been assumed that the entire neutron star core is superfluid. Our models will obviously still not be truly realistic, but we can (at least) compare results for different predicted superfluid energy gaps and varying neutron star core temperatures.

In order to determine to what extent the neutrons and protons are superfluid/superconducting at a given core temperature (assumed to be uniform), we will consider the phenomenological gap models discussed by Andersson, Comer & Glampedakis (2005). It is straightforward to use these models since they are given by analytic 'fits' to the original results. The only caveat is that the fits are not valid at very low temperatures. One should also be careful to use the analytic gap functions only in the density region where they are relevant.

We will compare r-mode results for two different models, intended to represent the range of possibilities. These models correspond to models [f,l] and [h,e] of Andersson et al. (2005) and represent what we will from now onwards refer to as 'strong' and 'weak' superfluidity, respectively. For our polytropic neutron star model, this leads to the critical temperatures (as functions of the radius) shown in Fig. 1. The results correspond to a model with mass $M = 1.4\,\mathrm{M}_\odot$ and radius $R = 10$ km (in the non-rotating limit). We take this as our canonical model. The data in Fig. 1 confirm the expectation that below a critical temperature the superfluid region will always be a shell, between to radii $R_{\rm min}(T)$ and $R_{\rm max}(T)$, where T is the core temperature. In order to simplify the analysis, we will only consider the core superfluids. This makes sense since we have not accounted for the elastic properties of the crust in the first place. Hence, we consider only the $^3P_2$ neutron superfluid and the $^1S_0$ proton superconductor. To model the fluid dynamics of this system, we make the usual assumption that protons and electrons are locked electromagnetically. This leads to the system exhibiting two-fluid dynamics only in the region where the neutrons are superfluid. When the neutrons are normal, scattering with the electrons will lock the neutron fluid to the charged components. Given these assumptions, the two-fluid region is such that $R_{\rm min}(T)$ corresponds to the inner $T = T_{\rm c}$ point for the neutron gap. Meanwhile, $R_{\rm max}(T)$ corresponds to either the outer $T = T_{\rm c}$ point or the crust–core transition ($R_{\rm c}$), whichever is the smallest. In our analysis we assume that the crust–core transition takes place at a density of $\rho = 1.6 \times 10^{14}\,\mathrm{g\,cm^{-3}}$ (Haensel 2001). For our canonical star, this leads to $R_{\rm c} \approx 9.32$ km.

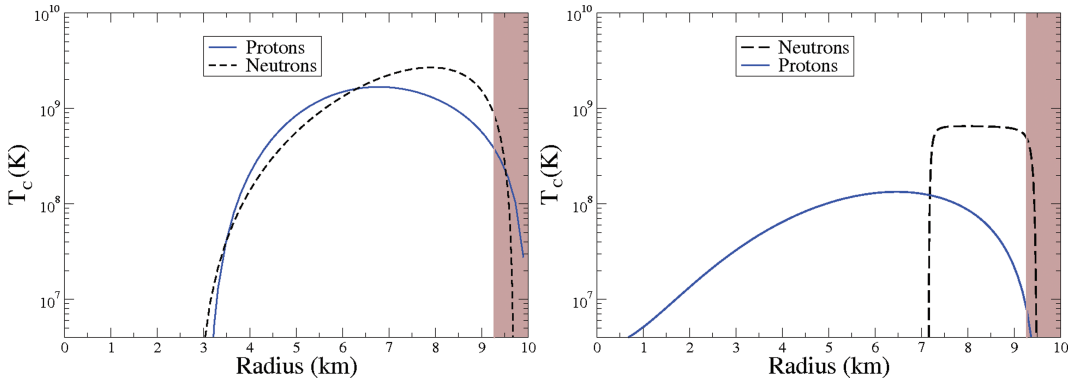

Figure 1. These figures show the critical temperatures for the onset of superfluidity of protons and neutrons as functions of radius in a stellar model with $M = 1.4\,\mathrm{M}_\odot$ and $R = 10$ km. We consider two models representing 'strong' (left-hand panel) and 'weak' (right-hand panel) superfluidity, respectively. For strong superfluidity we use models h and e of Andersson et al. (2005), while the weak superfluidity case corresponds to their models f and l. The shaded region indicates the crust, the dynamics of which are not accounted for in our r-mode calculation.

We need to impose boundary conditions on the two-fluid equations at $R_{\rm min}(T)$ and $R_{\rm max}(T)$. Following Lindblom & Mendell (2000) and Lee & Yoshida (2003), we take the pressure perturbation to be continuous at each interface. This ensures that it is consistent to use the analytic solution for the comoving part of the solution throughout the star. With these interface conditions, we require

$$\xi_-(R_{\rm min}) = 0 \quad \text{and} \quad \xi_-(R_{\rm max}) = 0. \tag{110}$$

Naturally, the r-mode mutual friction damping time will now depend on the size of the superfluid shell, i.e. the temperature of the star.

We also want to be able to make a direct comparison with the results of Lindblom & Mendell (2000) and Lee & Yoshida (2003). To do this, we consider a model such that the entire core is superfluid, with a critical density $\rho_{\rm s} = 2.8 \times 10^{14}\,\mathrm{g\,cm^{-3}}$, corresponding to a transition radius $R_{\rm s} \approx 8.85$ km in our model. We assume that the pressure perturbation is continuous at this interface, i.e. impose

$$\xi_-(R_{\rm s}) = 0. \tag{111}$$

The remaining condition in this case is regularity at the centre of the star.

4.5 The mutual friction damping time-scale

We will use the standard energy integral approach to assess the relative importance of different dissipation mechanisms and their impact on the r-mode instability. As discussed by, for example, Andersson et al. (2008), this analysis is based on a functional $E = E_{\rm k} + E_{\rm p}$, where $E_{\rm k}$ and $E_{\rm p}$ represent the 'kinetic' and 'potential' energy, respectively. In the non-dissipative case, the total energy is conserved. For the comoving r mode, the problem simplifies considerably. The potential energy is higher order in rotation than the kinetic energy, so all we need is

$$E \approx E_{\rm k} = \frac{1}{2}\int \rho \left[|\delta v|^2 + (1-\bar{\varepsilon})x_{\rm p}(1-x_{\rm p})|\delta w|^2\right] \mathrm{d}V. \tag{112}$$

As discussed by Andersson et al. (2008), the damping time-scale for a mode $\tau = -1/\Im(\omega)$ follows from

$$\frac{1}{\tau} = -\frac{1}{2E}\left(\frac{\mathrm{d}E}{\mathrm{d}t}\right). \tag{113}$$

Focusing on the mutual friction dissipation, we find from equations (11) and (15) that

$$\frac{\mathrm{d}E}{\mathrm{d}t} = -2\int \rho_{\rm n}\mathcal{B}\Omega\left[\delta_i^m - \hat{\Omega}^m\hat{\Omega}_i\right]\delta w^i \delta w_m^* \,\mathrm{d}V. \tag{114}$$

At the current level of approximation, we cannot determine the mutual friction damping of the classical r mode directly from the imaginary part of the mode frequency. This would require calculating the frequency up to the order of $O(\Omega^5)$, not $O(\Omega^3)$ as we have done here. This is easily seen if we note that, as the mode is purely comoving to the first order, $\delta v \approx O(\Omega)$ and $\delta w \approx O(\Omega^3)$. Thus, the energy scales as

$$E \approx (\delta v)^2 \approx O(\Omega^2) \quad \text{while} \quad \frac{\mathrm{d}E}{\mathrm{d}t} \approx \Omega(\delta w)^2 \approx O(\Omega^7)$$

and, from equation (113), we see that $\Im(\omega) \approx O(\Omega^5)$. This means that we, in fact, have to resort to the energy integral estimate. Since the evaluation, to leading order, of the integrals in (112) and (114) only requires the eigenfunctions up to the order of $O(\Omega^2)$, it can be performed within the present scheme. Due to the expected scaling, we will focus on the quantity τ_0 defined by the relation

$$\frac{1}{\tau} = \frac{1}{\tau_0}\left(\frac{\Omega}{\sqrt{\pi G\bar{\rho}}}\right)^5 \tag{115}$$

where $\bar{\rho}$ is the mean density of the star.

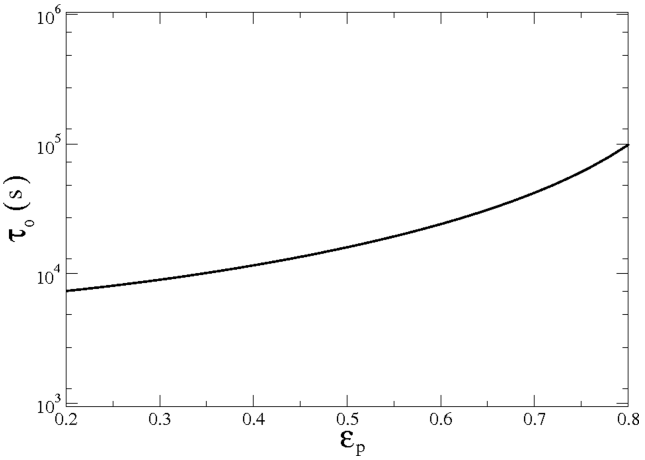

Figure 2. This figure shows the r-mode damping time-scale, τ_0, for a range of values of the entrainment parameter, ε_p. In order to facilitate a direct comparison with the results of Lindblom & Mendell (2000) and Lee & Yoshida (2003), we consider a model where the entire core is superfluid. The transition density is taken to be $\rho_s = 2.8 \times 10^{14}$ g cm^{-3}. The stellar model has mass $M = 1.4\,M_\odot$ and radius $R = 12.533$ km. We also assume that the mutual friction is due to electron scattering on vortex array, which gives $\mathcal{B}' \approx 0$ while $\mathcal{B}$ is obtained from equation (116). The absence of 'resonances', associating particular values of the entrainment with very short damping times, is notable in our results.

Having established the strategy, let us first of all consider the model where the superfluid extends all the way from the centre of the star up to R_s. In order to compare our results directly to Lindblom & Mendell (2000) and Lee & Yoshida (2003), we take the mass and radius of the star to be $M = 1.4\,M_\odot$ and $R = 12.533$ km. We also assume that the main cause of mutual friction is electron scattering off the vortex array. This assumption puts us firmly in the 'weak' drag regime where we can neglect the $\mathcal{B}'$ coefficient. Meanwhile, for $\mathcal{B}$ we have the result of Andersson et al. (2006);

$$\mathcal{B} = 4 \times 10^{-4} \left(\frac{m_p - m_p^*}{m_p} \right)^2 \left(\frac{m_p}{m_p^*} \right)^{1/2} \left(\frac{x_p}{0.05} \right)^{7/6} \left(\frac{\rho}{10^{14}\,\mathrm{g\,cm^{-3}}} \right)^{1/6}. \tag{116}$$

Results for the damping time-scale τ_0 due to mutual friction, with varying ε_p, are presented in Fig. 2. These results confirm the main conclusion of Lindblom & Mendell (2000) and Lee & Yoshida (2003). Mutual friction due to electron scattering off the vortex array is too weak to affect the r-mode instability significantly. There is, however, one important difference between our results and the previous studies. We do not find any value of ε_p for which the damping time-scale becomes short [cf. the resonances discussed by Lindblom & Mendell (2000) and Lee & Yoshida (2003)]. The absence of these resonances is most likely due to the fact that, following Andersson et al. (2008), we have imposed that the mode is purely axial to leading order. That is, we neglect higher-order terms that would couple the counter-moving motion back to the comoving motion. In effect, we have a priori ruled out the resonant behaviour found by Lindblom & Mendell (2000). Moreover, we cannot have avoided crossings with the superfluid inertial modes as discussed by Lee & Yoshida (2003). Once we assume that the r mode is purely axial to leading order, our analysis becomes completely oblivious to the fact that other mode solutions to the general problem may exist.

Another important difference between our analysis and the work of Lindblom & Mendell (2000) and Lee & Yoshida (2003) is that we explicitly keep the mutual friction terms in the equations of motion. The damping time-scale we calculate is obtained by using the full $O(\Omega^3)$ solution for the problem in the integral in equation (113), rather than integrating the solutions to the inviscid problem. In the weak drag limit, e.g. when we consider (116), this does not affect the results at all. However, by keeping the mutual friction force in the perturbed equations of motion we are no longer restricted to the weak drag limit. We can consider the entire range $0 \leq \mathcal{R} \leq \infty$. The capacity to consider the strong drag regime may, in fact, be quite important. Dynamics in the strong drag regime have only recently been considered (see e.g. Glampedakis et al. 2008), and the results show that the problem has interesting features. Hence, we will consider the r-mode problem outside the range $\mathcal{R} \ll 1$. Motivation for studying the problem for $\mathcal{R} \gg 1$ comes from the possibility that the interaction between fluxtubes and neutron vortices may be efficient (Ruderman et al. 1998; Link 2003, 2006). The problem would also be in this strong drag regime if a fluxtube cluster is associated with each neutron vortex (Sedrakian & Sedrakian 1995) or in the presence of strong vortex pinning (Shaham 1977).

Because of the 'symmetric' dependence of the mutual friction coefficient $\mathcal{B}$ on the drag $\mathcal{R}$, one may expect the damping time-scales to be similar for values $\mathcal{R}$ and $1/\mathcal{R}$. The damping should be most effective for $\mathcal{R} \approx 1$. The results in Fig. 3 illustrate the importance of keeping the mutual friction force terms in the perturbed equations of motion in this efficient friction regime. In the figure, we compare the mutual friction damping time-scale determined from the energy integral using eigenfunctions where we either keep both the $\mathcal{B}$ and the $\mathcal{B}'$ terms or (artificially) set one or both of them to zero. The evidence is clear. For $\mathcal{R} \approx 1$ the inviscid solution does no longer lead to a good approximation.

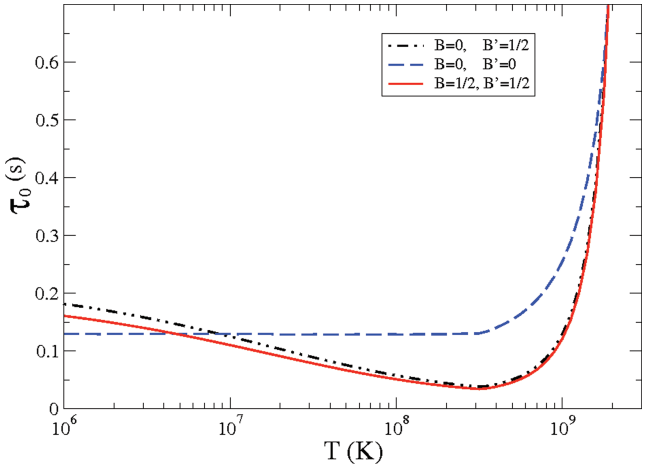

Figure 3. This figure shows the r-mode damping time-scale, τ_0, calculated for $\varepsilon_p = 0.6$ and $\mathcal{R} = 1$ for the strong superfluidity model. The results illustrate the importance of using the dissipative mode solution in the evaluation of the energy integrals. The dashed curve shows the time-scale obtained by integrating the undamped eigenfunctions. The other two curves show the effect of introducing first $\mathcal{B}'$ (dash–dot) and then also $\mathcal{B}$ (solid) in the calculation.

5 THE R-MODE INSTABILITY WINDOW FOR STRONG MUTUAL FRICTION

It is interesting to consider the case $\mathcal{R} \approx 1$ further, even though it is somewhat extreme (and possibly only of academic interest). After all, it leads to the strongest possible mutual friction damping. Moreover, because it corresponds to $\mathcal{B} \approx \mathcal{B}' \approx 1/2$, it provides insight into the dynamics of problems where the two terms in the mutual friction force are of similar importance.

Let us consider the effect that a strong mutual friction would have on the r-mode instability. To do this, we need to account for the various viscous processes which, at a given temperature, act to damp the gravitational-wave-driven instability. First of all, it is easy to see that the r modes will only be unstable in a certain temperature range. At temperatures below $T \approx 10^5$ K, shear viscosity will always suppress the instability, while for temperatures above $T \approx 10^{10}$ K (at which no part of the star is expected to be superfluid) bulk viscosity will prevent the mode from becoming unstable. Our aim is to establish to what extent the mutual friction can further restrict the range in which the mode is unstable.

The r-mode instability window is usually illustrated by the critical rotation period above which the mode is unstable as a function of temperature. The relevant critical rotation rate is obtained by solving for the roots of

$$\frac{1}{\tau_{\rm gw}} + \frac{1}{\tau_{\rm sv}} + \frac{1}{\tau_{\rm bv}} + \frac{1}{\tau_{\rm mf}} = 0 \tag{117}$$

where $\tau_{\rm gw}$ is the growth time-scale for the instability due to gravitational-wave emission. For an $n = 1$ polytrope, it is approximated by (Andersson & Kokkotas 2001)

$$\tau_{\rm gw} \approx -47 \left(\frac{M}{1.4\,{\rm M}_\odot}\right)^{-1} \left(\frac{R}{10\,{\rm km}}\right)^{-2l} \left(\frac{P}{1\,{\rm ms}}\right)^{2l+2} {\rm s}. \tag{118}$$

Even though this estimate was obtained for a single-fluid star, it will remain a good approximation for the ordinary r modes of a superfluid star. This is obvious since the gravitational-wave emission is entirely due to the comoving degree of freedom (Andersson et al. 2008). Meanwhile, $\tau_{\rm bv}$ represents the damping time due to bulk viscosity. The bulk viscosity will be suppressed in superfluid regions. Hence, it is only active in regions where the star is not superfluid. In general, this leads to a complex problem. However, in the case of npe-matter where only the modified Urca process is relevant the bulk viscosity damping is not important at low temperatures. Hence, we essentially only need the bulk viscosity at temperatures above the superfluid transition. That is, we use (Andersson & Kokkotas 2001)

$$\tau_{\rm bv} = 2.7 \times 10^{11} \left(\frac{M}{1.4\,{\rm M}_\odot}\right) \left(\frac{R}{10\,{\rm km}}\right)^{-1} \left(\frac{P}{1\,{\rm ms}}\right)^{2} \left(\frac{T}{10^9\,{\rm K}}\right)^{-6} {\rm s}. \tag{119}$$

It should be noted that the role of bulk viscosity will be different for hyperons and deconfined quarks because of a different scaling with temperature (see e.g. Nayyar & Owen 2006 for a recent discussion).

The damping time-scale, $\tau_{\rm mf}$, for mutual friction damping, and $\tau_{\rm sv}$, the time-scale for damping due to shear viscosity, require a more detailed discussion. In the case of mutual friction, we are interested in the temperature dependence of the damping time-scale. To investigate this, we consider the realistic gap models described in the previous section which, as they predict how the extent of the superfluid region varies with temperature, allow us to predict the temperature dependence of $\tau_{\rm mf}$ itself. Meanwhile, the shear viscosity damping also depends on which layers of the star are superfluid, as the dominant effect will be due to different processes in superfluid and normal fluid regions. In the region where the neutrons are not superfluid (the normal fluid region), we assume that the main contribution is due to neutron–neutron

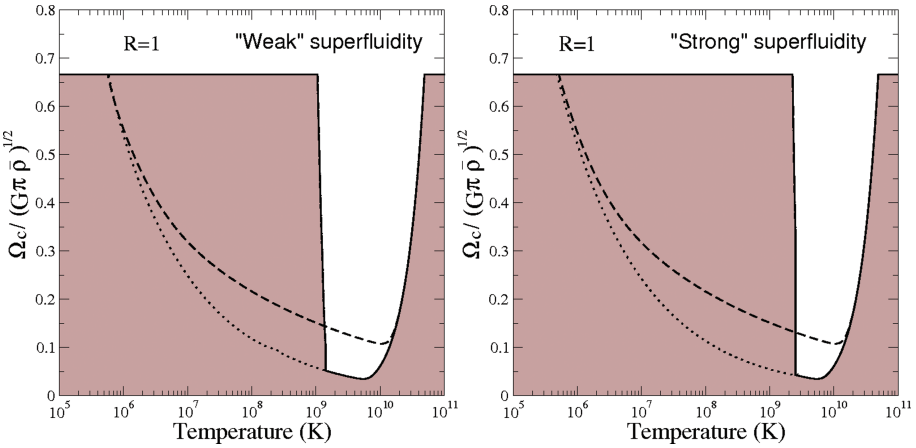

Figure 4. The r-mode instability window for $\varepsilon_p = 0.6$, calculated as a function of core temperature T and for $\mathcal{R} = 1$ in the 'weak' (left-hand panel) and 'strong' (right-hand panel) superfluidity cases. We consider a star with $M = 1.4\,\mathrm{M}_\odot$ and $R = 10$ km. The dotted line indicates the shape the instability window has if we ignore mutual friction, while the dashed line indicates the effect that the Ekman layer at the base of the crust would have on the instability region. The results show that, when $\mathcal{R} = 1$, the mutual friction is strong enough to suppress the r-mode instability completely as soon as the core becomes superfluid.

scattering. This leads to a viscosity coefficient (Andersson & Kokkotas 2001)

$$\eta_{\rm nn} = 2 \times 10^{18} \left(\frac{\rho}{10^{15}\,\mathrm{g\,cm^{-3}}}\right)^{9/4} \left(\frac{T}{10^9\,\mathrm{K}}\right)^{-2} \mathrm{g\ cm^{-1}\,s^{-1}}. \tag{120}$$

If only the neutrons are superfluid, then the dominant process will be electron–proton scattering which leads to the coefficient (Andersson et al. 2005)

$$\eta_{\rm ep} = 1.8 \times 10^{16} \left(\frac{x_{\rm p}}{0.01}\right)^{13/6} \left(\frac{\rho}{10^{15}\mathrm{g\,cm^{-3}}}\right)^{13/6} \left(\frac{T}{10^9\,\mathrm{K}}\right)^{-2} \mathrm{g\ cm^{-1}\,s^{-1}}. \tag{121}$$

If, on the other hand, *both* neutrons and protons are superfluid, the dominant process is electron–electron scattering (Andersson et al. 2005), which leads to the coefficient (Andersson & Kokkotas 2001)

$$\eta_{\rm ee} = 6 \times 10^{18} \left(\frac{\rho}{10^{15}\,\mathrm{g\,cm^{-3}}}\right)^{2} \left(\frac{T}{10^9\,\mathrm{K}}\right)^{-2} \mathrm{g\ cm^{-1}\,s^{-1}}. \tag{122}$$

Once we have determined the dominant viscosity agent in each region of the star, we can compute the damping time-scale from the energy integral

$$\left[\frac{\mathrm{d}E}{\mathrm{d}t}\right]_{\rm sv} = -2\int \eta \delta\sigma^{ab}\delta\sigma^*_{\rm ab}\,\mathrm{d}V \tag{123}$$

where the shear $\delta\sigma_{\rm ab}$ is defined as

$$\delta\sigma_{\rm ab} = \frac{i\omega}{2}\left(\nabla_a\xi^+_b - \nabla_b\xi^+_a - 2g_{\rm ab}\nabla_{\rm c}\xi^c_+\right). \tag{124}$$

The obtained results for the instability window are shown in Figs 4–6for a range of drag parameters in the $\mathcal{R} \approx 1$ regime, and the 'strong' and 'weak' superfluidity models. The data correspond to an $M = 1.4\,\mathrm{M}_\odot$ and $R = 10$ km neutron star. In the figures, we express the critical angular velocity in terms of $\Omega_0 = \sqrt{\pi G\bar{\rho}}$ where $\bar{\rho}$ is the average density, and assume that the star cannot spin faster than the breakup limit, taken to be $\Omega_{\rm b} \approx 2/3\Omega_0$.

Note that, as we are considering a purely fluid star and do not account explicitly for the elastic crust we have not included the damping time-scale due to the Ekman layer which is expected to form at the crust–core boundary. To indicate the effect that the Ekman layer may have on the instability window, we use the rough estimate

$$\tau_{\rm Ek} = 3 \times 10^5 \left(\frac{T}{10^9\,\mathrm{K}}\right)\left(\frac{P}{1\,\mathrm{ms}}\right)^{1/2} \mathrm{s}. \tag{125}$$

We arrive at this estimate by taking the simple constant density estimate of Andersson & Kokkotas (2001) for an $M = 1.4\,\mathrm{M}_\odot$ and $R = 10$ km neutron star, corrected for a 'slippage' factor $\mathcal{S}_{\rm c} = 0.05$, as defined by Glampedakis & Andersson (2006b). In fact, it has been shown by Glampedakis & Andersson (2006a) that one should expect the constant density estimate to only differ by factors of a few from the result for a stratified model. Hence, it should be a reasonable approximation for our discussion.

Perhaps not very surprisingly, our analysis demonstrates that the mutual friction damping can have a significant effect on the r-mode instability window in the extreme case $\mathcal{R} \approx 1$. It is, however, interesting to note the impact on the instability window of the two superfluidity models. The results in Figs 5 and 6 show that, for values of the drag parameter in the range $0.005 < \mathcal{R} < 500$, mutual friction may have a significant effect on the r-mode instability. Comparing the two figures, we see that the 'strong' or 'weak' superfluidity models lead to significantly different results in the strong friction regime (keeping the mass and radius of the star fixed). As the star cools below the superfluid

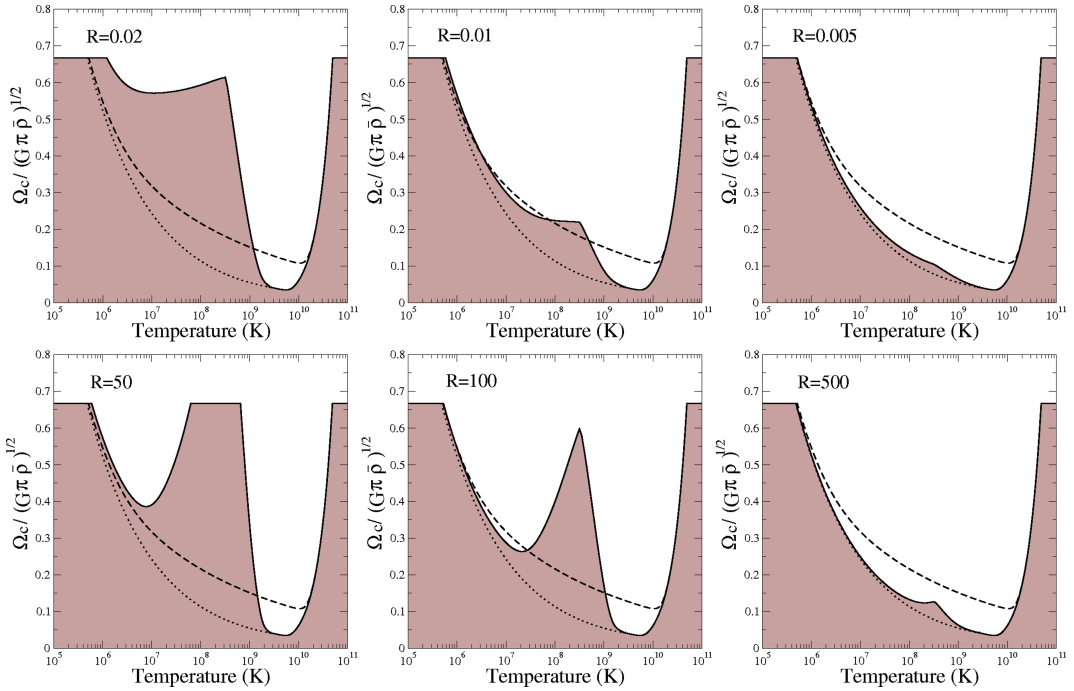

Figure 5. The r-mode instability window for $\varepsilon_p = 0.6$, calculated as a function of core temperature T and for a range of drag parameters $\mathcal{R}$. We consider a star with $M = 1.4\,M_\odot$ and $R = 10$ km and 'strong' superfluidity. The dotted line indicates the shape the instability window has if we ignore mutual friction, while the dashed line indicates the effect that the Ekman layer at the base of the crust would have on the instability region. The results show that, for values of the drag parameter in the range $0.005 < \mathcal{R} < 500$, mutual friction may have a significant effect on the r-mode instability. It is particularly interesting to note the local minimum that may be present at low temperatures. This feature arises due to the effect shown in Fig. 3.

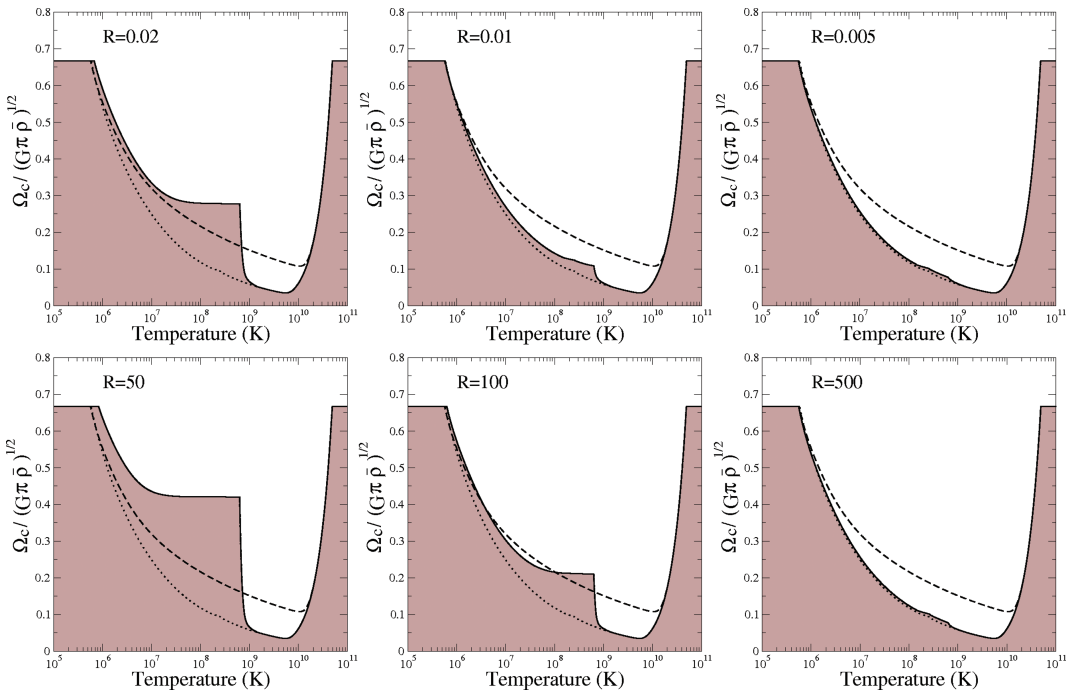

Figure 6. Same as Fig. 5, but for the 'weak' superfluidity model.

transition temperature, the mutual friction time-scale initially decreases (the critical frequency increases). However, at lower temperatures the damping time may increase again (around $T \approx 10^9$ K). This would lead to a second minimum in the instability curve. For parameter values outside the range $0.005 < \mathcal{R} < 500$, the mutual friction would not be the dominant dissipation mechanism for the superfluid r modes.

It should be stressed that we have focused on cases where both $\mathcal{B}'$ and $\mathcal{B}$ are relevant. In the very strong drag regime (i.e. $\mathcal{R} \gg 1$), one will have $\mathcal{B}' \approx 1$ but $\mathcal{B} \ll 1$. In this limit, one again finds that the mutual friction damping of the r modes is irrelevant.

6 CONCLUDING REMARKS

In this paper, we have re-examined the problem of mutual friction damping in rotating superfluid neutron stars and its effect on the r-mode instability. Our analysis differed from previous efforts in that we did not a priori assume that the drag on the superfluid vortices is weak. By including the mutual friction force in the equations of motion, we were able to (for the first time) consider r modes in the strong drag regime. We calculated these modes to second order in rotation, thus extending the first-order results of Andersson et al. (2008).

Our mode analysis focused on solutions that are purely axial to leading order. For the classical r mode, which is expected to lead to the fastest growing gravitational-wave instability, this assumption has the advantage that the equations for the comoving degree of freedom decouple and serve as source for the counter-moving motion in the superfluid region of the star. For the particular case of an $n = 1$ polytrope, and in the Cowling approximation, we determined a useful analytic solution for the comoving motion. The existence of this solution, which is relevant also for the single-fluid barotropic r mode, simplified the solution of the superfluid problem considerably.

In the superfluid problem, there may also exist a class of counter-moving r modes. These modes are, however, in general not purely axial to leading order. For a stratified neutron star model, the velocity field of these modes acquire a leading order polar component. Such modes cannot be determined within our current framework. This means that we cannot confirm the proposed existence of 'avoided crossings' between the two classes of modes. Such crossings have been suggested as the explanation for the sharp resonances with very short mutual friction damping time-scales found by Lindblom & Mendell (2000) and Lee & Yoshida (2003). Our results do not show such resonances. Whether this is an artefact of our approximation scheme is not clear. We see no evidence that our approximation fails for particular values of the entrainment, as one might expect if the r modes change character as the entrainment is varied. This issue requires further attention.

We have, however, calculated the counter-moving r mode in the only case where it can exist, when the star is not stratified (see Appendix B). In this case, it is possible to obtain, once again, an analytic solution. This solution, which was presented here for the first time, has already been used as a test bench for numerical simulations of superfluid neutron stars (Passamonti et al. 2008).

For the classical (mainly comoving) r mode, our results confirm that mutual friction due to the most commonly considered mechanism (electron scattering off the vortex array) acts on a time-scale that is too long to suppress the r-mode instability. We conclude that, in the weak drag regime, the mutual friction is not the leading damping mechanism for these modes. This agrees with the conclusions of Lindblom & Mendell (2000) and Lee & Yoshida (2003).

We have also considered, for the first time, the effect of the mutual friction on r modes in the strong drag regime. In the extreme limit, this leads to the expected result that the damping time-scale is (again) very long. Hence, mutual friction does not damp r modes effectively in the $\mathcal{R} \gg 1$ regime. In order to understand the effect that a strong mutual friction may have, we have also studied the intermediate regime where $\mathcal{R} \approx 1$, when $\mathcal{B}' \approx \mathcal{B} \approx 1/2$. This regime could be relevant if there exists regions in the star where the interaction between neutron vortices and fluxtubes is efficient (Ruderman et al. 1998; Link 2003, 2006). In this case, we find that mutual friction can have a distinct effect on the r-mode instability window. The instability may, in fact, be completely suppressed below the superfluid transition temperature. Moreover, the mutual friction damping depends strongly on the model for the superfluid energy gap, which determines the critical temperature below which neutrons or protons become superfluid. We have compared results for two typical models, taken from Andersson et al. (2005), representing 'strong' and 'weak' superfluidity, respectively. This analysis lays the foundation for studies of realistic neutron star models, where the size of the superfluid regions depends explicitly on the stars temperature.

With this analysis, we have prepared the ground for a more detailed study of neutron stars with exotic cores, e.g. dominated by hyperons or deconfined quarks. In each of these cases, one would expect superfluidity to be relevant. In the case of hyperons, the problem is likely to require additional 'fluid' degrees of freedom. Naively, one would expect the neutron and proton superfluid/superconducting mixture to coexist with a neutral Λ superfluid and a Σ^- superconductor. Assuming electromagnetic coupling between the charged components, this would leave three distinct hydrodynamical degrees of freedom (at zero temperature). Neutron stars with deconfined quark cores may also require additional degrees of freedom. Perhaps the simplest possibility corresponds to the so-called Colour Flavor Locked (CFL) phase (Alford et al. 1999) for which, at low temperatures, one has to consider a superfluid coupled to phonon excitations (Mannarelli, Manuel & Sa'd 2008). This should lead to a dynamical problem that is formally equal to superfluid He^4 (see Andersson & Comer 2008 for a recent discussion). More complicated phases, requiring the inclusion of Kaons, either as thermal excitations or as a condensate, will also need to be considered. It would be very interesting, and perhaps important, to understand better to what extent multifluid dynamics play a role for such exotic systems.

ACKNOWLEDGMENTS

This work was supported by STFC in the UK through grant number PP/E001025/1.

REFERENCES

Alford M. G., Rajagopal K., Wilczek F., 1999, Nucl. Phys. B, 537, 443
Alpar M. A., Langer S. A., Sauls J. A., 1984, ApJ, 282, 533
Andersson N., 1998, ApJ, 502, 708
Andersson N., Comer G. L., 2001, MNRAS, 328, 1129
Andersson N., Comer G. L., 2006, Class. Quantum. Grav., 23, 5505
Andersson N., Comer G. L., 2008, preprint (arXiv:0811.1660)

Andersson N., Kokkotas K. D., 2001, Int. J. Mod. Phys. D, 10, 381
Andersson N., Kokkotas K. D., Schutz B. F., 1999a, ApJ, 510, 846
Andersson N., Kokkotas K. D., Stergioulas N., 1999b, ApJ, 516, 307
Andersson N., Comer G. L., Glampedakis K., 2005, Nucl. Phys. A, 763, 212
Andersson N., Sidery T., Comer G. L., 2006, MNRAS, 368, 162
Andersson N., Sidery T., Comer G. L., 2007, MNRAS, 381, 747
Andersson N., Glampedakis K., Haskell B., 2008, Phys. Rev. D, 79, 103009
Bildsten L., 1998, ApJ, 501, L89
Chamel N., 2008, MNRAS, 388, 737
Chandrasekhar S., 1933, MNRAS, 93, 390
Glampedakis K., Andersson N., 2006a, MNRAS, 371, 1311
Glampedakis K., Andersson N., 2006b, Phys. Rev. D, 74, 044040
Glampedakis K., Andersson N., 2008, preprint (arXiv:0806.3664)
Glampedakis K., Andersson N., Jones D. I., 2008, Phys. Rev. Lett., 100, 081101
Glampedakis K., Andersson N., Jones D. I., 2009, MNRAS, 394, 1908
Haensel P., 2001, in Blaschke D., Glendenning N. K., Sedrakian A., eds, Neutron Star Crusts., LNP Vol. 578, Springer Verlag, New York, p. 127
Lee U., 1995, A&A, 303, 515
Lee U., Yoshida S., 2003, ApJ, 586, 403
Lindblom L., Mendell G., 1994, ApJ, 421, 689
Lindblom L., Mendell G., 1995, ApJ, 444, 804
Lindblom L., Mendell G., 2000, Phys. Rev. D, 61, 104003
Lindblom L., Mendell G., Owen B. J., 1999, Phys. Rev. D, 60, 64006
Link B., 2003, Phys. Rev. Lett., 91, 101101
Link B., 2006, A&A, 458, 881
Mannarelli M., Manuel C., Sa'd B. A., 2008, Phys. Rev. Lett., 101, 241101
Nayyar M., Owen B. J., 2006, Phys. Rev. D, 73, 084001
Passamonti A., Haskell B., Andersson N., 2008, MNRAS, in press (arXiv:0812.3569)
Peralta C., Melatos A., Giacobello M., Ooi A., 2005, ApJ, 635, 1224
Peralta C., Melatos A., Giacobello M., Ooi A., 2006, ApJ, 651, 1079
Prix R., 2004, Phys. Rev. D, 69, 043001
Prix R., Rieutord M., 2002, A&A, 393, 949
Prix R., Comer G. L., Andersson N., 2004, MNRAS, 348, 625
Ruderman M., Zhu T., Chen K., 1998, ApJ, 492, 267
Saio H., 1982, ApJ, 256, 717
Sedrakian A. D., Sedrakian D. M., 1995, ApJ, 447, 305
Shaham J., 1977, ApJ, 214, 251
Smeyers P., Martens L., 1983, A&A, 125, 193
Tassoul J. L., 1978, Theory of Rotating Stars. Princeton University Press, Princeton
Watts A. L., Krishnan B., Bildsten L., Schutz B. F., 2008, MNRAS, 389, 839
Yoshida S., Lee U., 2000, ApJS, 129, 353

APPENDIX A: DERIVING THE R-MODE EQUATIONS

In this Appendix, we provide the derivation of the equations that determine the rotational corrections to the r modes. We take as our starting point the general slow-rotation perturbation equations from Section 3.1. Focusing on modes that are purely toroidal to leading order, we assume that the total displacement vector takes the form

$$\frac{\xi^i_+}{a} = \left(0, \frac{K_{lm}}{\sin\theta}\frac{\partial}{\partial\phi}, -K_{lm}\frac{\partial}{\partial\theta}\right) Y^m_l + \sum_{\nu,\mu}\left(S_{\nu\mu}, Z_{\nu\mu}\frac{\partial}{\partial\theta}, \frac{Z_{\nu\mu}}{\sin\theta}\frac{\partial}{\partial\phi}\right) Y^\mu_\nu. \tag{A1}$$

Meanwhile, the difference displacement vector can be written as

$$\frac{\xi^i_-}{a} = \left(0, \frac{k_{lm}}{\sin\theta}\frac{\partial}{\partial\phi}, -k_{lm}\frac{\partial}{\partial\theta}\right) Y^m_l + \sum_{\nu,\mu}\left(s_{\nu\mu}, z_{\nu\mu}\frac{\partial}{\partial\theta}, \frac{z_{\nu\mu}}{\sin\theta}\frac{\partial}{\partial\phi}\right) Y^\mu_\nu. \tag{A2}$$

We use uppercase variables for the comoving degree of freedom and the corresponding lowercase variable for the counter-moving degree of freedom.

Our main interest is in the 'classical' $l = m$ r mode, a mode that to the first order in rotation involves only the comoving degree of freedom and which is purely toroidal. This leads to the requirement that the leading term K_{lm} is of the order of unity while the amplitude of the spheroidal components is of the order of Ω^2 for the total displacement. Moreover, the first-order results of Andersson et al. (2008) show that all components of the difference displacement must be of the order of Ω^2. With this ordering for the displacement vector, and for the frequency given in equation (53), we have the equations

$$\begin{aligned}\sum_{\nu,\mu} a\frac{\mathrm{d}S_{\nu\mu}}{\mathrm{d}a}Y^\mu_\nu = &\sum_{\nu,\mu}\left[\left(\frac{V}{\Gamma}-3\right)S_{\nu\mu} - \frac{V}{\Gamma_1}\zeta_{\nu\mu} + \nu(\nu+1)Z_{\nu\mu}\right]Y^\mu_\nu \\ &+ 3imK_{lm}\left(3D_2 + a\frac{\mathrm{d}D_2}{\mathrm{d}a}\right)\cos\theta Y^m_l\end{aligned} \tag{A3}$$

$$\sum_{\nu,\mu} a\frac{\mathrm{d}\zeta_{\nu\mu}}{\mathrm{d}a}Y_\nu^\mu = \sum_{\nu,\mu}\left[(1-U)\zeta_{\nu\mu} - \frac{V}{\Gamma}x_{\rm p}\tau_{\nu\mu}\right]Y_\nu^\mu - 2ic_1\omega\tilde{\omega}K_{lm}\sin\theta\frac{\partial Y_l^m}{\partial\theta}. \tag{A4}$$

These relations follow from the equations for the total displacement, (11) and (13). From the corresponding equations for the difference, i.e. (15) and (19), we get

$$\sum_{\nu,\mu} a\frac{\mathrm{d}s_{\nu\mu}}{\mathrm{d}a}Y_\nu^\mu = \sum_{\nu,\mu}\left[(X-3)s_{\nu\mu} - \zeta_{\nu\mu}\frac{1}{(1-x_{\rm p})}\frac{V}{\Gamma} + \nu(\nu+1)z_{\nu\mu} - CS_{\nu\mu}\right]Y_\nu^\mu \tag{A5}$$

$$\begin{aligned}\sum_{\nu,\mu} a\frac{\mathrm{d}\tau_{\nu\mu}}{\mathrm{d}a}Y_\nu^\mu = \sum_{\nu,\mu}\Bigg[&(1-U)\tau_{\nu\mu}Y_\nu^\mu - 2k_{lm}c_1\omega\tilde{\omega}\left(i\bar{\mathcal{B}}'\sin\theta\frac{\partial Y_l^m}{\partial\theta} - m\bar{\mathcal{B}}\cos\theta Y_l^m\right) - 2c_1\omega\tilde{\omega}z_{\nu\mu}\left(m\bar{\mathcal{B}}' + i\bar{\mathcal{B}}\sin\theta\cos\theta\frac{\partial Y_\nu^\mu}{\partial\theta}\right)\\ &+ c_1\omega s_{\nu\mu}\left(\omega(1-\bar{\varepsilon})Y_\nu^\mu + 2i\tilde{\omega}\bar{\mathcal{B}}(\cos^2\theta-1)Y_\nu^\mu\right)\Bigg].\end{aligned} \tag{A6}$$

In writing down these equations, we have defined the variables

$$\sum_{\nu,\mu}\zeta_{\nu\mu}Y_\nu^\mu = \frac{1}{ga}\left(\frac{\delta p}{\rho}\right) \tag{A7}$$

$$\sum_{\nu,\mu}\tau_{\nu\mu}Y_\nu^\mu = \frac{1}{ga}\delta\beta. \tag{A8}$$

The various background quantities are defined by equations (70)–(77).

Combining the θ and ϕ components of the comoving Euler equation, we also obtain two algebraic relations

$$\sum_{\nu,\mu}\nu(\nu+1)\zeta_{\nu\mu}Y_\nu^\mu + 2ic_1\omega\tilde{\omega}K_{lm}\left[l(l+1)\cos\theta Y_l^m + \sin\theta\frac{\partial Y_l^m}{\partial\theta}\right] = 0 \tag{A9}$$

and

$$\begin{aligned}&K_{lm}\omega\left\{l(l+1)(1+2\epsilon)(\omega-\omega_0)Y_l^m + 6D_2\left[\omega\cos\theta\sin\theta\frac{\partial Y_l^m}{\partial\theta} - m\tilde{\omega}(5\cos\theta^5-1)Y_l^m\right]\right\}\\ &-2i\omega\tilde{\omega}\sum_{\nu,\mu}\left\{\left[2S_{\nu\mu}-\nu(\nu+1)Z_{\nu\mu}\right]\cos\theta Y_\nu^\mu + (S_{\nu\mu}-Z_{\nu\mu})\sin\theta\frac{\partial Y_\nu^\mu}{\partial\theta}\right\} = 0\end{aligned} \tag{A10}$$

where

$$\omega_0 = \frac{2m\tilde{\omega}}{l(l+1)}. \tag{A11}$$

Analogously, we obtain from the difference Euler equations

$$\begin{aligned}\sum_{\nu,\mu}\nu(\nu+1)\tau_{\nu\mu}Y_\nu^\mu = &-2ic_1\bar{\mathcal{B}}'\omega\tilde{\omega}k_{lm}\left[l(l+1)\cos\theta Y_l^m + \sin\theta\frac{\partial Y_l^m}{\partial\theta}\right] + 2m\bar{\mathcal{B}}c_1\omega\tilde{\omega}k_{lm}\left[2\cos\theta Y_l^m + \sin\theta\frac{\partial Y_l^m}{\partial\theta}\right]\\ &+c_1\omega\sum_{\nu,\mu}z_{\nu\mu}\left[\omega\nu(\nu+1)(1-\bar{\varepsilon})Y_\nu^\mu - 2\tilde{\omega}m\bar{\mathcal{B}}'Y_\nu^\mu - 2i\tilde{\omega}\bar{\mathcal{B}}(m^2Y_\nu^\mu + \nu(\nu+1)\cos^2\theta Y_\nu^\mu + 2\sin\theta\cos\theta\frac{\partial Y_\nu^\mu}{\partial\theta})\right]\\ &-2c_1\omega\tilde{\omega}\sum_{\nu,\mu}s_{\nu\mu}\left\{m\bar{\mathcal{B}}'Y_\nu^\mu - i\bar{\mathcal{B}}\left[\cos\theta\sin\theta\frac{\partial Y_\nu^\mu}{\partial\theta} + (3\cos^2\theta-1)Y_{\mu\nu}\right]\right\}\end{aligned} \tag{A12}$$

and

$$\begin{aligned}k_{lm}\omega l(l+1)(1+2\varepsilon)(1-\bar{\varepsilon})(\omega-\omega_1)Y_l^m = &2i\omega\tilde{\omega}\sum_{\nu,\mu}\left[(2\bar{\mathcal{B}}' - im\bar{\mathcal{B}})s_{\nu\mu} - \bar{\mathcal{B}}'\nu(\nu+1)z_{\nu\mu}\right]\cos\theta Y_\nu^\mu\\ &+\sum_{\nu,\mu}[\bar{\mathcal{B}}'s_{\nu\mu} - (\bar{\mathcal{B}}' - im\bar{\mathcal{B}})z_{\nu\mu}]\sin\theta\frac{\partial Y_\nu^\mu}{\partial\theta}\end{aligned} \tag{A13}$$

where

$$\omega_1 = \frac{\tilde{\omega}}{l(l+1)(1-\bar{\varepsilon})}\{2m\bar{\mathcal{B}}' + 2i\bar{\mathcal{B}}\left[l(l+1)-m^2\right]\}. \tag{A14}$$

We can now use the standard recurrence relations

$$\sin\theta\frac{\partial Y_l^m}{\partial\theta} = lQ_{l+1}Y_{l+1}^m - (l+1)Q_lY_{l-1}^m \tag{A15}$$

$$\cos\theta Y_l^m = Q_{l+1}Y_{l+1}^m + Q_lY_{l-1}^m \tag{A16}$$

with Q_l defined in (79). Repeated use of these relations leads to

$$\cos\theta \sin\theta \frac{\partial Y_l^m}{\partial \theta} = \left[l Q_{l+1}^2 - (l+1) Q_l^2\right] Y_l^m + l Q_{l+1} Q_{l+2} Y_{l+2}^m - (l+1) Q_l Q_{l-1} Y_{l-2}^m \tag{A17}$$

$$\cos^2\theta Y_l^m = \left(Q_{l+1}^2 + Q_l^2\right) Y_l^m + Q_{l+1} Q_{l+2} Y_{l+2}^m + Q_l Q_{l-1} Y_{l-2}^m. \tag{A18}$$

This way we arrive at the equations that determine the next-order slow-rotation correction to the $l = m$ r mode;

$$a\frac{\mathrm{d}S_{l+1}}{\mathrm{d}a} = \left(\frac{V}{\Gamma} - 3\right) S_{l+1} - \frac{V}{\Gamma}\zeta_{l+1} + (l+1)(l+2) Z_{l+1} + 3im Q_{l+1} K_{lm} \left(3D_2 + a\frac{\mathrm{d}D_2}{\mathrm{d}a}\right) \tag{A19}$$

$$a\frac{\mathrm{d}\zeta_{l+1}}{\mathrm{d}a} = (1-U)\zeta_{l+1} - \frac{V}{\Gamma} x_\mathrm{p} \tau_{l+1} - 2ic_1 \omega\tilde{\omega} l Q_{l+1} K_{lm} \tag{A20}$$

$$a\frac{\mathrm{d}s_{l+1}}{\mathrm{d}a} = (X-3)\, s_{l+1} - \zeta_{l+1} \frac{1}{x_\mathrm{p}(1-x_\mathrm{p})} \frac{V}{\Gamma} + (l+1)(l+2) z_{l+1} - C S_{l+1} + 3im Q_{l+1} k_{lm} \left(3D_2 + a\frac{\mathrm{d}D_2}{\mathrm{d}a}\right) \tag{A21}$$

$$\begin{aligned} a\frac{\mathrm{d}\tau_{l+1}}{\mathrm{d}a} &= (1-U)\tau_{l+1} - 2c1\omega\tilde{\omega} Q_{l+1} k_{lm} \left(il\bar{\mathcal{B}}' - m\bar{\mathcal{B}}\right) - 2c_1\omega\tilde{\omega} z_{l+1} \left\{m\bar{\mathcal{B}}' + i\bar{\mathcal{B}}\left[(l+1)Q_{l+2}^2 - (l+2)Q_{l+1}^2\right]\right\} \\ &\quad + c_1 \omega s_{l+1} \left\{\omega(1-\bar{\varepsilon}) + 2i\tilde{\omega}\bar{\mathcal{B}}\left[\left(Q_{l+2}^2 + Q_{l+1}^2\right) - 1\right]\right\} \end{aligned} \tag{A22}$$

$$\zeta_{l+1} = -2i\omega\tilde{\omega} c_1 \frac{l}{l+1} Q_{l+1} K_{lm} \tag{A23}$$

$$\begin{aligned} \tau_{l+1}(l+1)(l+2) &= -2i\bar{\mathcal{B}}'\omega\tilde{\omega} c_1 l(l+2) Q_{l+1} k_{lm} + 2m(l+2)\bar{\mathcal{B}}\omega\tilde{\omega} c_1 Q_{l+1} k_{lm} \\ &\quad + c_1\omega z_{l+1}\left\{\omega(l+1)(l+2)(1-\bar{\varepsilon}) - 2m\tilde{\omega}\bar{\mathcal{B}}' - 2i\tilde{\omega}\bar{\mathcal{B}}\left[m^2 + Q_{l+2}^2(l+1)(l+4) + Q_{l+1}^2(l+2)(l-1)\right]\right\} \\ &\quad - 2c_1\omega\tilde{\omega} s_{l+1}\left\{m\bar{\mathcal{B}}' - i\bar{\mathcal{B}}\left[Q_{l+2}^2(l+4) - Q_{l+1}^2(l-1) - 1\right]\right\} \end{aligned} \tag{A24}$$

where

$$K_{lm} = -\frac{i\omega_0}{me} l Q_{l+1}\left[S_{l+1} + (l+2) Z_{l+1}\right] \tag{A25}$$

$$k_{lm} = \frac{\omega_0}{m\eta}\left(m\bar{\mathcal{B}} - il\bar{\mathcal{B}}'\right) Q_{l+1}\left[s_{l+1} + (l+2) z_{l+1}\right]. \tag{A26}$$

In the last two expressions, we have used

$$e = (\omega - \omega_0) + 3D_2 \left\{\frac{2\omega}{l+1} Q_{l+1}^2 - \omega_0\left[5Q_{l+1}^2 - 1\right]\right\} \tag{A27}$$

$$\eta = (1-\bar{\varepsilon})(\omega_0 - \omega_1). \tag{A28}$$

The above equations are identical (58)–(68) in Section 4.1. They completely specify the r-mode problem at second-order slow rotation.

APPENDIX B: THE COUNTER-MOVING R MODE

In this Appendix, we will examine the 'superfluid' r mode, a mode that to the first order in rotation involves only the counter-moving degrees of freedom and which is purely toroidal. This leads to the requirement that the leading term k_{lm} is of the order of unity while the amplitudes of the spheroidal components are of the order of Ω^2 for the difference displacement. Moreover, all the components of the total displacement are of the order of Ω^2. We have already mentioned that such a mode cannot exist unless the proton fraction is constant (Andersson et al. 2008). Nevertheless, these modes may be of some interest. Hence, it is worth determining the relevant slow-rotation corrections.

Given the ordering for the displacement vector, together with the frequency from (53), we have the following equations (for the $l = m$ mode):

$$a\frac{\mathrm{d}S_{l+1}}{\mathrm{d}a} = \left(\frac{V}{\Gamma} - 3\right) S_{l+1} - \frac{V}{\Gamma}\zeta_{l+1} + (l+1)(l+2) Z_{l+1} \tag{B1}$$

$$a\frac{\mathrm{d}\zeta_{l+1}}{\mathrm{d}a} = (1-U)\zeta_{l+1} - \frac{V}{\Gamma} x_\mathrm{p} \tau_{l+1} - 2ic_1\omega\tilde{\omega} l Q_{l+1} K_{lm} \tag{B2}$$

$$a\frac{\mathrm{d}s_{l+1}}{\mathrm{d}a} = (X-3)\, s_{l+1} - \eta_{l+1} + (l+1)(l+2) z_{l+1} - C S_{l+1} + 3im Q_{l+1} k_{lm} \left(3D_2 + a\frac{\mathrm{d}D_2}{\mathrm{d}a}\right) \tag{B3}$$

$$a\frac{\mathrm{d}\tau_{l+1}}{\mathrm{d}a} = (1-U)\tau_{l+1} - 2c_1\omega\tilde{\omega} Q_{l+1} k_{lm}\left(il\bar{\mathcal{B}}' - m\bar{\mathcal{B}}\right) \tag{B4}$$

$$\zeta_{l+1} = -2i\omega\tilde{\omega}c_1\frac{l}{l+1}Q_{l+1}K_{\rm lm} + c1z_{l+1}\left[\omega - \frac{2}{(l+1)(l+2)}\tilde{\omega}\right] - \frac{2m}{(l+1)(l+2)}c_1\omega\tilde{\omega}S_{l+1}$$
$$\tau_{l+1} = -2i\bar{\mathcal{B}}'\omega\tilde{\omega}c_1\frac{l}{(l+1)}Q_{l+1}k_{lm} + 2\frac{m}{(l+1)}\bar{\mathcal{B}}\omega\tilde{\omega}c_1Q_{l+1}k_{lm} \tag{B5}$$

and

$$K_{lm} = -\frac{i\omega_0}{me}lQ_{l+1}\left[S_{l+1} + (l+2)Z_{l+1}\right] \tag{B6}$$

$$k_{lm} = \frac{\omega_0}{m\eta}\left(m\bar{\mathcal{B}} - il\bar{\mathcal{B}}'\right)Q_{l+1}\left[s_{l+1} + (l+2)z_{l+1}\right] \tag{B7}$$

where

$$e = (\omega - \omega_0) \tag{B8}$$

$$\eta = (1-\bar{\varepsilon})(\omega_0 - \omega_1) + 3D_2\left\{\frac{2\omega(1-\bar{\varepsilon})}{l(l+1)}\left[lQ_{l+1}^2 - (l+1)Q_l^2\right] - \omega_0\left[5Q_{l+1}^2 + 5Q_l^2 - 1\right]\right\} \tag{B9}$$

and we have defined the variable

$$\sum_{\nu,\mu}\eta_{\nu\mu}Y_\nu^\mu = \frac{1}{x_{\rm p}\left(1-x_{\rm p}\right)}\delta x_{\rm p}. \tag{B10}$$

We can now show that one cannot in general have a pure counter-moving r mode, as in this case one has k_{lm} of the order of unity and, thus from equation (B6) one finds that τ_{lm} is of the order of Ω^2. This means that in equation (B2) the terms involving ζ_{lm} must be of the same order, but this would lead, from equation (B5), to one or more components of the total displacement vector being of the order of unity. The mode would thus no longer be a pure counter-moving r mode, but a more general inertial mode. However, this argument fails if we assume constant density profile. In this case, there is no coupling term in equation (B2) and one can solve the problem by defining an enthalpy-type variable (see Andersson et al. 2008).

Hence, we consider an equation of state for which the two fluids are decoupled. In particular, we shall consider the analytical equation of state of Prix et al. (2004) and Passamonti et al. (2008). Then, the energy functional takes the form

$$\mathcal{E} = \frac{1}{2}A_{\rm xy}\rho_{\rm x}\rho_{\rm y}\,, \tag{B11}$$

where $A_{\rm xy}$ is given by

$$A_{\rm nn} = \frac{2K}{1-(1+\sigma)\,x_{\rm p}}\,, \qquad A_{\rm pp} = \frac{2K[1+\sigma-(1+2\sigma)x_{\rm p}]}{x_{\rm p}[1-(1+\sigma)x_{\rm p}]}\,, \qquad A_{\rm np} = -\sigma\,A_{\rm nn}\,, \tag{B12}$$

and $x_{\rm p}, \sigma$ and K are constants. In the background, one has $p = K\rho^2$ and a constant proton fraction, while for the perturbations one finds that

$$\delta P = 2K\rho\,\delta\rho\,, \qquad \delta\beta = \frac{2K\,(1+\sigma)}{x_{\rm p}[1-(1+\sigma)x_{\rm p}]}\rho\delta x_{\rm p}\,. \tag{B13}$$

We now see that the coupling term in equation (19) vanishes, as $x_{\rm p}$ is constant, and there is also no coupling from the equation of state as (i) the pressure is a function of the density only, and (ii) β is a function of $x_{\rm p}$ only.

Let us consider the inviscid problem. This is of immediate interest since we can test the solution against the recent time-evolutions carried out by Passamonti et al. (2008). Neglecting the mutual friction, the equations for the mode we are interested in take the form

$$a\frac{{\rm d}s_{l+1}}{{\rm d}a} = (X-3)s_{l+1} + (l+1)(l+2)z_{l+1} + \frac{V}{\Gamma}E\tau_{l+1} \tag{B14}$$

$$a\frac{{\rm d}\tau_l + 1}{{\rm d}a} = (1-U)\tau_{l+1} - 2ic_1\omega\tilde{\omega}Q_{l+1}lT_l \tag{B15}$$

where

$$E = \frac{1+x_{\rm p}(1+\sigma)}{(1-x_{\rm p})(1+\sigma)}. \tag{B16}$$

The equations for the comoving degree of freedom are completely decoupled and take the same form as in equations (90) and (92). The frequency of the counter-moving r mode can be written as

$$\sigma^s = \sigma_0^s\Omega + \sigma_2^s\Omega^3 \tag{B17}$$

with (Andersson et al. 2008)

$$\sigma_0^s = \frac{1}{(1-\bar{\varepsilon})}\frac{2m}{l(l+1)}. \tag{B18}$$

In order to determine the correction σ_2^s, we adopt the same strategy as for the classical r mode and use the solution to equation (B14) to find a particular solution to equation (B15). Skipping the details of the calculation, which is essentially the same as in Section 4.3, we obtain the

relation

$$\sigma_2^s = -\frac{16}{\pi^2}\frac{l}{(l+1)^4(2l+3)}\left[\frac{\pi^{2l+5}}{2(2l+5)}E - \frac{5\pi^2(l+1)^2}{8}f_2(\pi)\right]\frac{1}{\mathcal{I}_2(1-\bar{\varepsilon})^2}. \tag{B19}$$

Here, we have assumed that the entire star is superfluid, and imposed the boundary condition $\Delta\beta = 0$ at the surface, in order to be able to compare directly to the numerical results of Passamonti et al. (2008). This comparison leads to a very good agreement [see fig. 2 of Passamonti et al. (2008)].

This paper has been typeset from a TEX/LATEX file prepared by the author.